RSC Advances

ROYAL SOCIETY OF CHEMISTRY

www.rsc.org/advances

Titania Nanostructures: A Biomedical Perspective

Vinod B. Damodaran,*[a] Divya Bhatnagar,[a] Victoria Leszczak,[b,c] and Ketul C. Popat*[b]

[a]New Jersey Center for Biomaterials and Rutgers – The State University of New Jersey, Piscataway, NJ-08854, USA.

[b]Department of Mechanical Engineering and School of Biomedical Engineering, Colorado State University, Fort Collins, CO-80523, USA.

[c]Present Address: United States Patent and Trademark Office (USPTO), Alexandria, VA, USA. (**Disclaimer:** The views and opinions presented in this article are solely those of the author and do not necessarily represent those of the USPTO.)

*E-mail: vinod.damodaran@rutgers.edu (VBD); ketul.popat@colostate.edu (KCP)

TOC

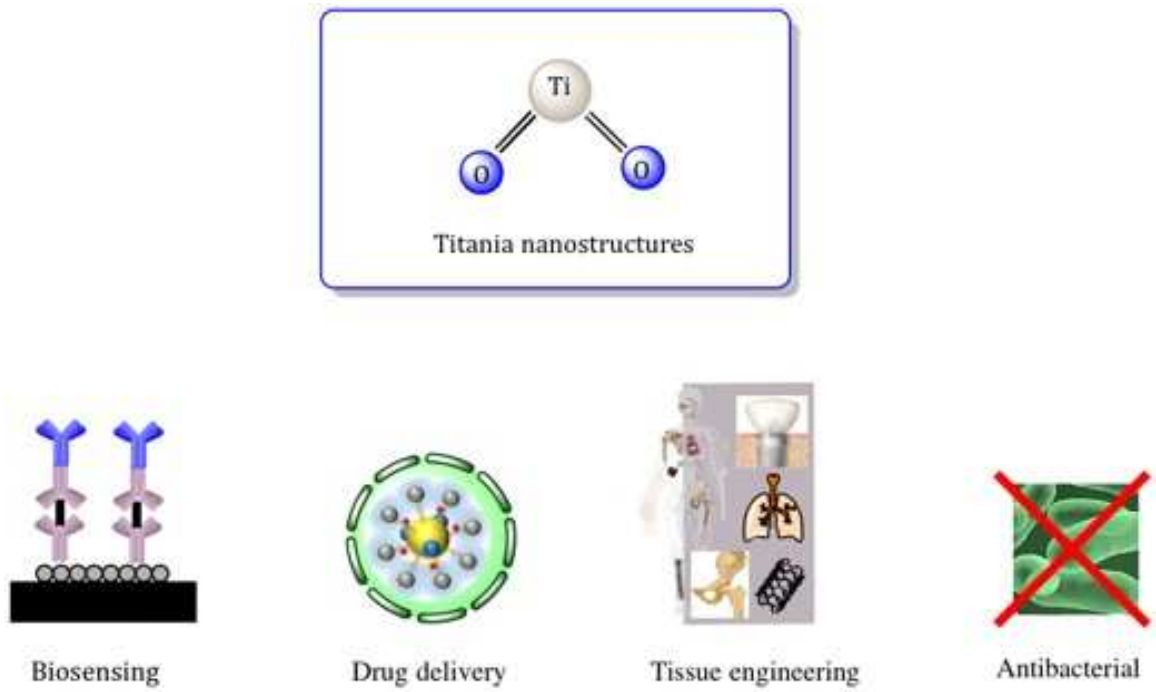

A systematic and comprehensive summary of various TNS-based biomedical research with a special emphasis to drug-delivery, tissue engineering, biosensor, and anti-bacterial applications.

Abstract

Titania nanostructures (TNSs) provides an exceptional choice for developing innovative biomedical applications due to their unique and characteristic biocompatibility, and their ability to integrate functional moieties to modulate biological responses. In this review, we provided first-hand knowledge of all contemporary TNS-based biomedical research for future innovations and benefits to the society and patient care. Starting with a brief discussion on the crystallographic phases of TNSs, we presented a detailed description of the commonly used fabrication and surface modification techniques, followed by a systematic and comprehensive summary of various biomedical evaluations with a special emphasis to drug-delivery, tissue engineering, biosensor, and anti-bacterial applications.

1. Introduction

Since the disclosure of the electrochemical photolysis of water using semiconducting titania (titanium dioxide, TiO_2) electrodes by Fujishima and Honda[1] in early 1970s, titania has become one of the most attractive and studied metal-oxide systems by various material scientists. Because of the characteristic stability, excellent mechanical, photocatalytic, and semiconducting properties; titania materials have found a wide variety of utilities ranging from energy to environmental applications.[2-5] Improvements in the nanotechnology research has resulted in fabrication of various forms of titania nanostructures (TNSs), such as nanotubes, nanowires, nanorods, nanobelts, and nanoribbons, with enhanced surface area and various size aspect ratios. These titania

nanostructures have attracted much interest in biomedical field due to their unique and characteristic compatibility with the biological system, and their ability to integrate functional moieties on the surface that can modulate biological responses.

Facilitated by the government and private sector interest and funding,[6] there are tremendous initiatives currently in progress globally to develop technologies and devices to improve the quality of health and patient care. Furthermore, caused by an increase in the aging world population, an increase in demand for such novel healthcare devices and services are anticipating in the coming decades. Consequently, a substantial growth of market potential is expected for the global medical device industry from the previously reported market value of $350 billion in 2012.[7] Tapping this potential, TNSs provide an exceptional choice for developing such innovative biomedical applications with enhanced biocompatibility and functionality.

In this review, we aimed to provide first-hand knowledge of all contemporary TNSs-based biomedical research for future innovations and benefit to the society and patient care. We begin with a brief discussion on the crystallographic phases of TNSs with a detailed discussion of the commonly using fabrication and surface modification methods. In the subsequent sections, we present a systematic and comprehensive summary of various biomedical evaluations with a special emphasis to tissue engineering, drug-delivery, biosensor, and anti-bacterial applications (Fig. 1).

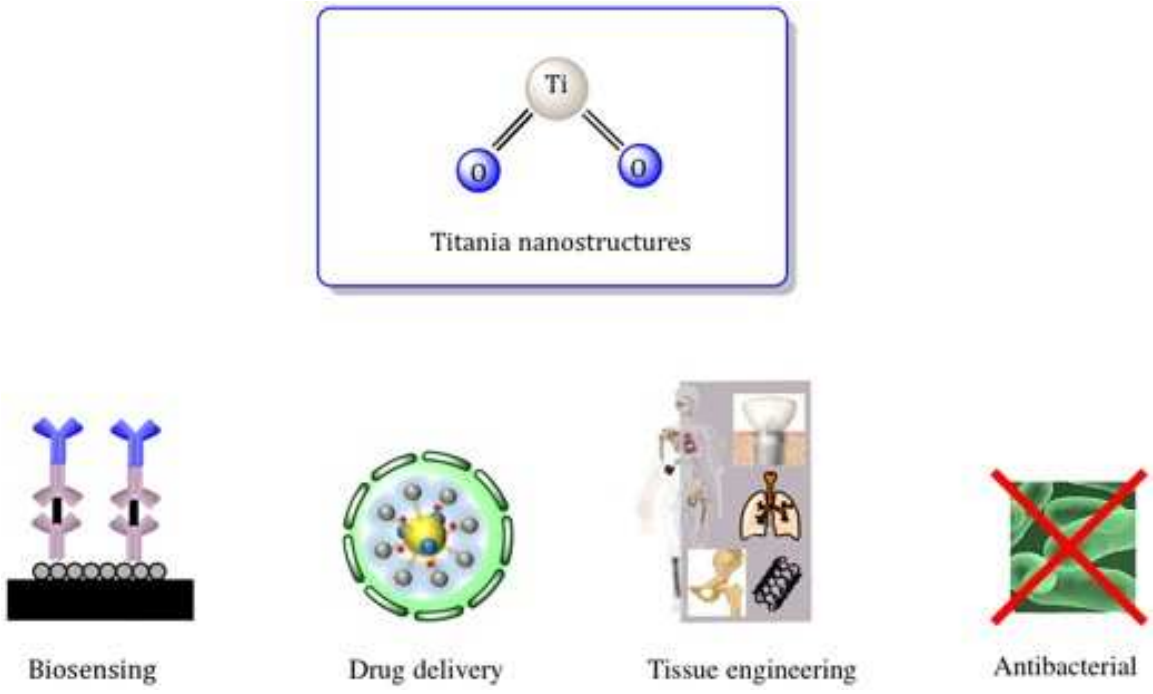

Fig. 1 Schematic illustration of various biomedical applications of TNSs described in this review article.

2. Crystallographic phases

TiO_2 can exist in one of the three naturally crystallographic phases, namely anatase, rutile, and brookite or a synthetically layered phase named as TiO_2-B (Fig. 2).[8] X-ray diffraction studies including extended X-ray absorption fine structure (EXAFS) and X-ray absorption near-edge spectroscopy (XANES) suggests a distorted TiO_6 octahedron combination with different symmetries for all these phases.[9] Among these, rutile is the most stable phase, and all other metastable phases can transform into this stable rutile form at high temperature depending on the environment and aging.[10, 11] While the

majority of the TNSs exhibit either rutile or anatase crystalline phases, the successful synthesis of various TNSs with TiO_2-B phase is also reported.[12-15] However, even though the exact crystalline phase of various TNSs is still a matter of scientific dispute, which requires stringent and systematic investigation, the observed phase can be greatly dependent on the starting material, synthesis, and drying conditions.

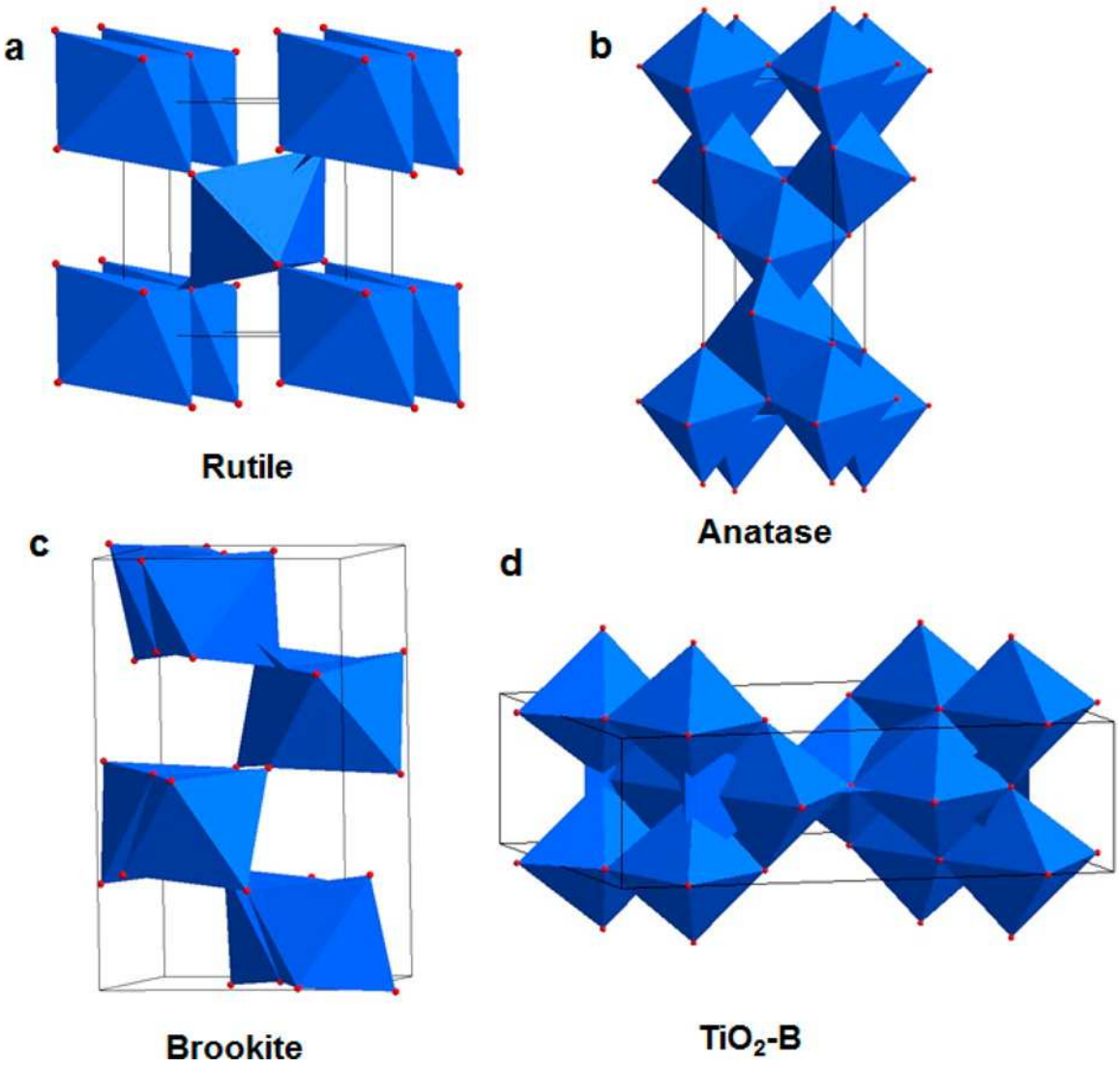

Fig. 2 Schematic unit cell structure of four TiO_2 crystallographic phases. Reproduced with permission from Ref [8] © American Chemical Society.

3. Synthesis

Template-assisted, electrochemical, and hydrothermal methods are the three major approaches to synthesize various nanostructural forms of titania. A brief description of these three methods, along with some interesting approaches, is presented in the following sections.

3.1 Template-assisted

Template-assisted methods provide an attractive strategy for fabricating well-defined titania nanostructures in large quantities with controlled dimensions and monodispersity.[16, 17] In this method, TiO_2 is prepared in situ by controlled sol-gel hydrolysis of a Ti-based precursor, and allowed to deposit or polymerize onto a template, that results in the reproduction of the template morphology. The template used can be either positive or negative.[18] With a positive template, TiO_2 is deposited outside of the template structure; while with a negative template, TiO_2 is deposited inside the template structure. Finally, the template can be selectively removed by chemical or solvent etching, and annealed at about 500°C to generate titania nanostructures. However even though well-defined and diameter-controllable nanostructures can be prepared by this technique, damage to nanostructures during the template removal and residual template material contaminations are the serious drawbacks associated with this method.[19]

Because of the highly ordered pore structures, uniform pore-size, controllable pore geometry, and high surface area, anodic aluminum oxide (AAO)[18] with nanoporous architecture is the most commonly used template method for preparing various TNSs. The very first attempt to prepare titania nanotube array using AAO template material was reported by Hoyer in mid 1990s.[20] Polycrystalline anatase samples were prepared by electrochemical deposition of TiO_2 onto an AAO based template followed by template dissolution and heat treatment. This method has successfully translated to the synthesis of various well-defined and highly ordered single as well as multi-walled TNSs by many researchers (Fig. 3).[20-27]

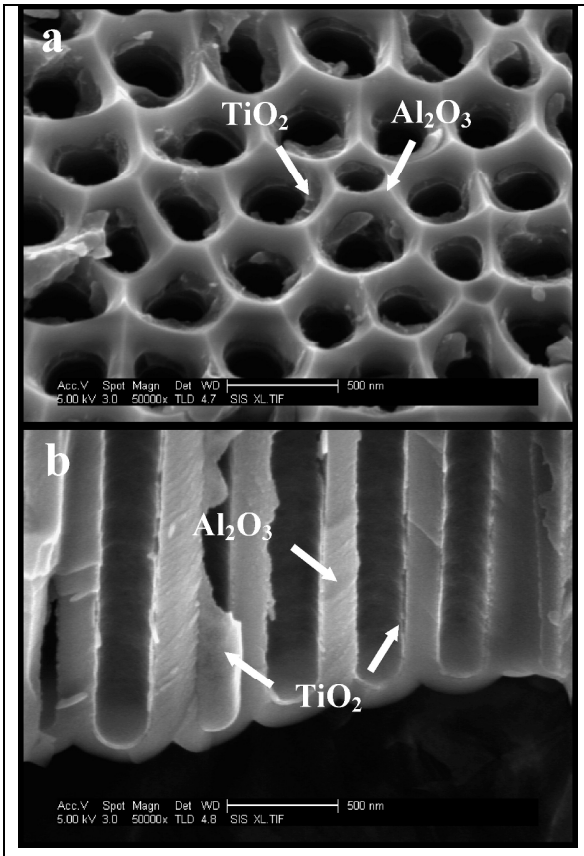

Fig. 3a Field emission−SEM images of (a) top-down and (b) cross-sectional views of

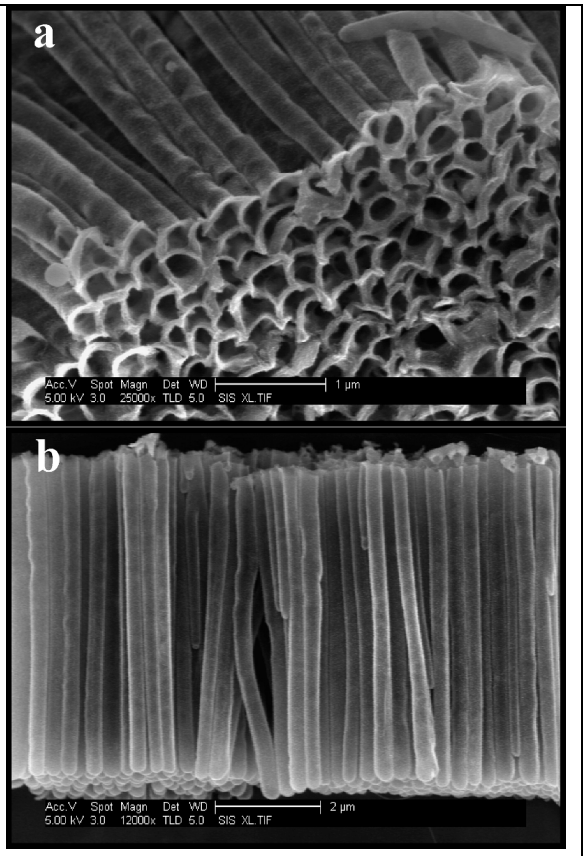

Fig. 3b Field emission−SEM images of (a) top-down and (b) side views of TiO_2

an alumina template after infiltration and annealing at 500 °C for 30 min. The average nanopore diameter and TiO_2 wall thickness are 295 and 21 nm, respectively. Reproduced with permission from Ref. [21] © American Chemical Society.	nanotube arrays after removal of the anodized alumina template. The average TiO_2 nanotube outer diameter and length are 295 nm and 6.1 μm, respectively. Reproduced with permission from Ref. [21] © American Chemical Society.

Sacrificial carbon nanotubes,[28-30] zinc oxide (ZnO),[31, 32] and self-assembled organic surfactants[33, 34] are also often used as template materials for preparing TNSs. Recently Li et al.[35] successfully synthesized hierarchically assembled and interconnected TNSs using a porous carbon nanotube (CNT) sponge as the template. This fabrication process involved the transformation of a hydrophobic CNT sponge, prepared via a chemical vapor deposition method, to titania nanotubular macrostructure through an intermediate core-shell TiO_2-CNT sponge. Using a hydrothermally grown branched ZnO nanorod template, Moonoosawmy et al.[32] prepared three-dimensionally branched titania nanotubes on a silicon substrate. Selective removal of the sacrificial ZnO template followed by annealing at 350°C resulted in self-standing, branched anatase titania nanotubes having 6 μm length and 600 nm width with approximate 65 nm wall thickness. Laurylamine hydrochloride[33], trans-(1R,2R)-1,2-Cyclohexanedi(11-aminocarbonylundecylpyridinium) organogel,[34] and tripodal cholamide-based hydrogel[36] are some of the examples of organic surfactant template commonly used for synthesizing TNSs.

3.2 Electrochemical

Electrochemical anodization offers a cost-effective and relatively simple method to prepare TNSs with uniform orientation and high aspect ratio. In general, anodization is

performed in a two-electrode system with titanium as the anode and a platinum cathode in presence of a fluoride ion-containing electrolyte. The mechanism of growth is a selective etching involving an anodic titanium oxide formation (eq. 1), followed by the chemical dissolution as a soluble hexafluorotitanate complex (eq. 2), and effusion of the complex.[37, 38]

$$Ti + 2H_2O \rightarrow TiO_2 + 4H^+ + 4e^- \quad (1)$$

$$TiO_2 + 6F^- + 4H^+ \rightarrow [TiF_6]^{2-} + 2H_2O \quad (2)$$

Enhanced and localized dissolution of the initially formed titanium oxide, under the influence of an applied electric field, results in the nucleation of nanopores at the surface. Subsequently, a steady-state pore growth on the metal surface is observed, facilitated by the simultaneous dissolution of $[TiF_6]^{2-}$ and the migration of TiO_2 into the substrate, leading to the formation of tubular geometries (Fig. 4).[39, 40] The dimensions and geometries of TNSs prepared by this technique can be conveniently controlled by varying the applied voltage, electrolyte composition, pH, and anodizing time.[40-42]

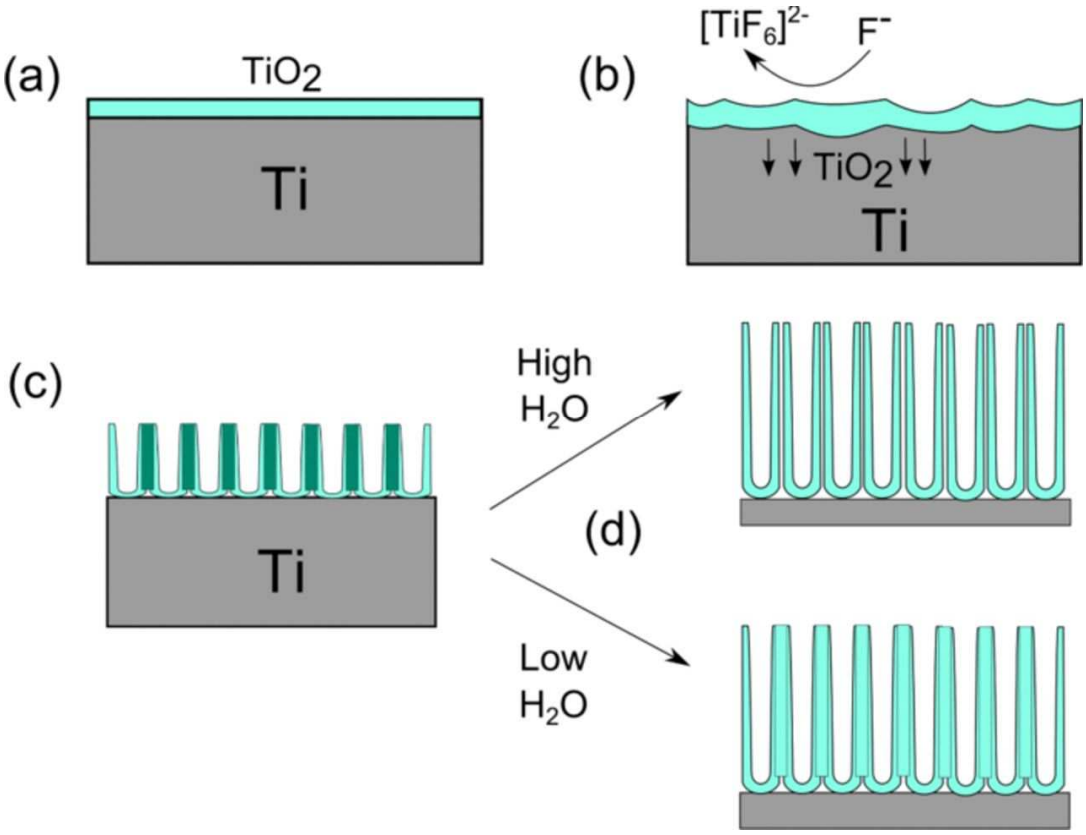

Fig. 4 Formation process of TiO_2 nanotubes. (a) Initial compact layer of TiO_2 formed by anodization. (b) attack by F- ions and propagation of TiO_2 further into the substrate. (c) disorganized pore layer is formed with gaps filled in. (c) In the presence of sufficient water, the interior is dissolved and separated tubes are formed. Reproduced from Ref [39] © Tsui and Zangari, under the terms of the Creative Commons Attribution Non-Commercial No Derivatives 4.0 License.

This technique was first reported by Gong et al. in 2001 for preparing self-organized titania nanotubular arrays using anodic oxidation of a titanium substrate in 0.5 to 3.5 wt% hydrofluoric acid aqueous solution.[43] Following this, many researchers explored the electrochemical anodization technique as their primary choice for making various TNSs (Fig. 5).[44-48]

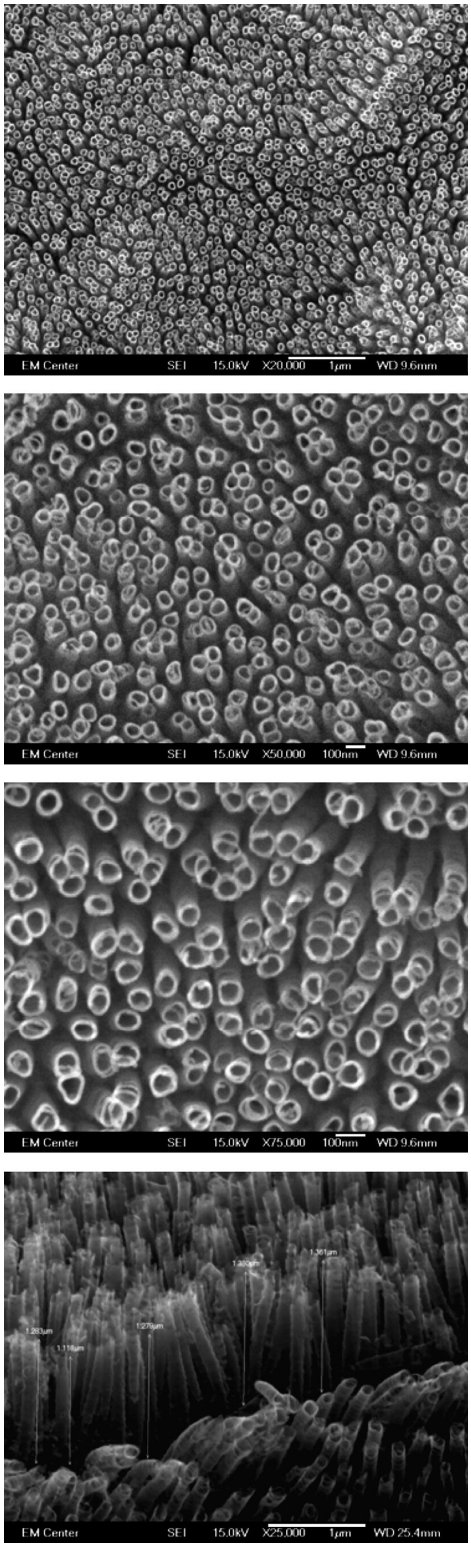

Fig. 5 Representative SEM images showing the nanoarchitecture (20,000×, 50,000×, 75,000× magnification) and the length of titania nanotube arrays (25,000×) prepared by

the electrochemical anodizaton process. Titania nanotube arrays were coated with a 10 nm layer of gold and imaged at 15 keV. Reproduced with permission from Ref. [47] © Elsevier.

3.3 Hydrothermal

Alkaline hydrothermal method offers a convenient, cost-effective and scalable route to prepare various TNSs, including nanotubes,[49-51] nanobelts,[52, 53] nanorods,[53] and nanowires,[54] based on alkaline treatment of a suitable titanium oxide precursor.[55-57] In 1998, Kasuga et al.[58] first reported the synthesis of needle-shaped titania nanotubes by an alkaline hydrothermal method by treating a sol-gel derived TiO_2-SiO_2 powder with a 5-10 M NaOH solution at 110°C. The formation mechanism of nanotubes, proposed by Kasuga et al. [59] starts with the breaking of some Ti-O-Ti bonds in the presence of NaOH, which results in the formation of Ti-O-Na and Ti-OH bonds. In the subsequent washing process with hydrochloric acid, Ti-O-Na bonds will be protonated to produce Ti-O-H. During the dehydration process, Ti-O-H bonds will be converted into either Ti-O-Ti or the hydrogen bonded Ti-O-H-O-Ti species. During this process, a reduction in the distance between the two surface Ti atoms will occur. This results in the folding of sheets and ultimately leads to the formation of tubular geometries through the connection between the ends of sheets. However, the rate of formation and morphology of the TNSs produced by this technique are greatly influenced by the nature of the initial material, reaction temperature, time, and NaOH concentration.[60-62] Recently Chien et al.[63] demonstrated that TNSs with different morphologies can be conveniently prepared from the same precursor by changing the hydrothermal temperature and time. Starting with a commercially available titanium dioxide precursor in 12M NaOH solution, the

researchers successfully synthesized titania nanotubes, nanorods, and nanowires at 140 °C/24h, 180 °C/24h, and 180 °C/72h respectively.

With an additional ethanol treatment to the intermediates prepared from the alkaline hydrothermal method, Ni et al.[64] improved the anatase crystallinity and photocatalytic activity of the fabricated nanobelts, compared to the non-treated specimens (Fig. 6). A novel vapor-phase hydrothermal approach for the direct growth of vertically aligned titanate nanotubes on a titanium substrate was reported by Liu et al. in 2011.[65] Contrary to the typical liquid-phase alkaline method, which produces nanotubes with about 12 nm external diameters, this process produced nanotubes having larger dimensions with external diameters of 50–80 nm and walls with an average thickness of 10 nm. Using a water–dichloromethane interface-assisted hydrothermal method, Wang et al.[66] successfully promoted the selective radial growth of densely packed rutile titania nanowires on electrospun anatase TiO_2 nanofibers to form a branched heterojunction architecture. In summary, the hydrothermal method is well adapted by many nanotechnologists and provides a versatile technique to prepare TNSs with various morphologies.

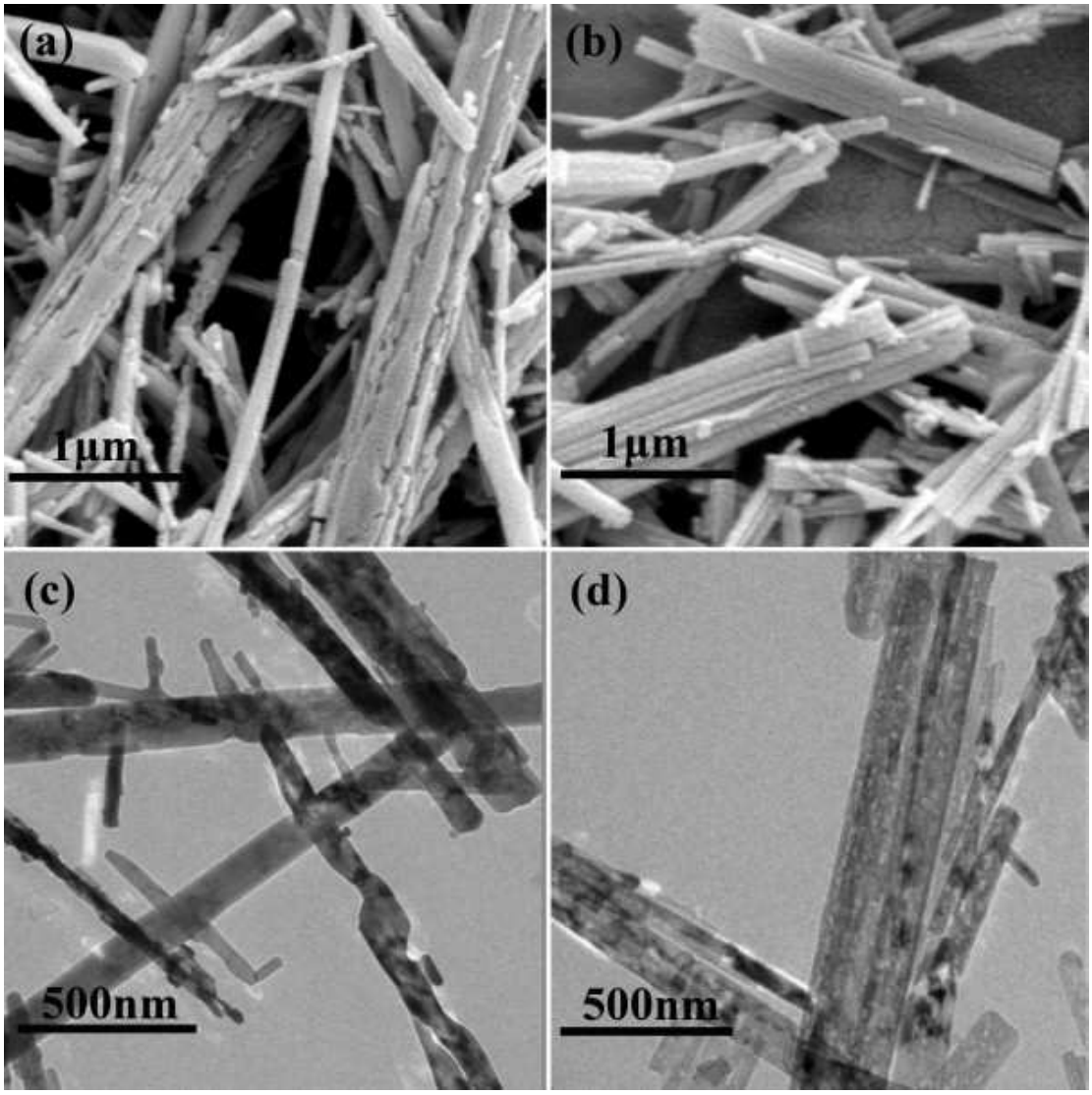

Fig. 6 Field emission-SEM images of the TiO_2 nanobelts with (a) and without ethanol treatment of (b); respective TEM images (c) and (d). Ni et al. Reproduced with permission from Ref [64] © Elsevier.

3.4 Miscellaneous approaches

Among other fabrication methods, many researchers explored electrospinning technique quite frequently for preparing TNSs with large aspect ratios. Anatase titania nanotubes with diameters of 20-200 nms were prepared by Li and Xia[67] by electrospinning an

ethanol-acetic acid solution of titanium tetraisopropoxide (TTIP) and polyvinyl pyrrolidone (PVP) (Fig. 7). Later researchers showed that, the morphology and dimensions of the electrospun TNSs can be conveniently altered by changing the applied electric field, titania precursor and solubilizer concentrations, solvent, and the input rate.[68, 69]

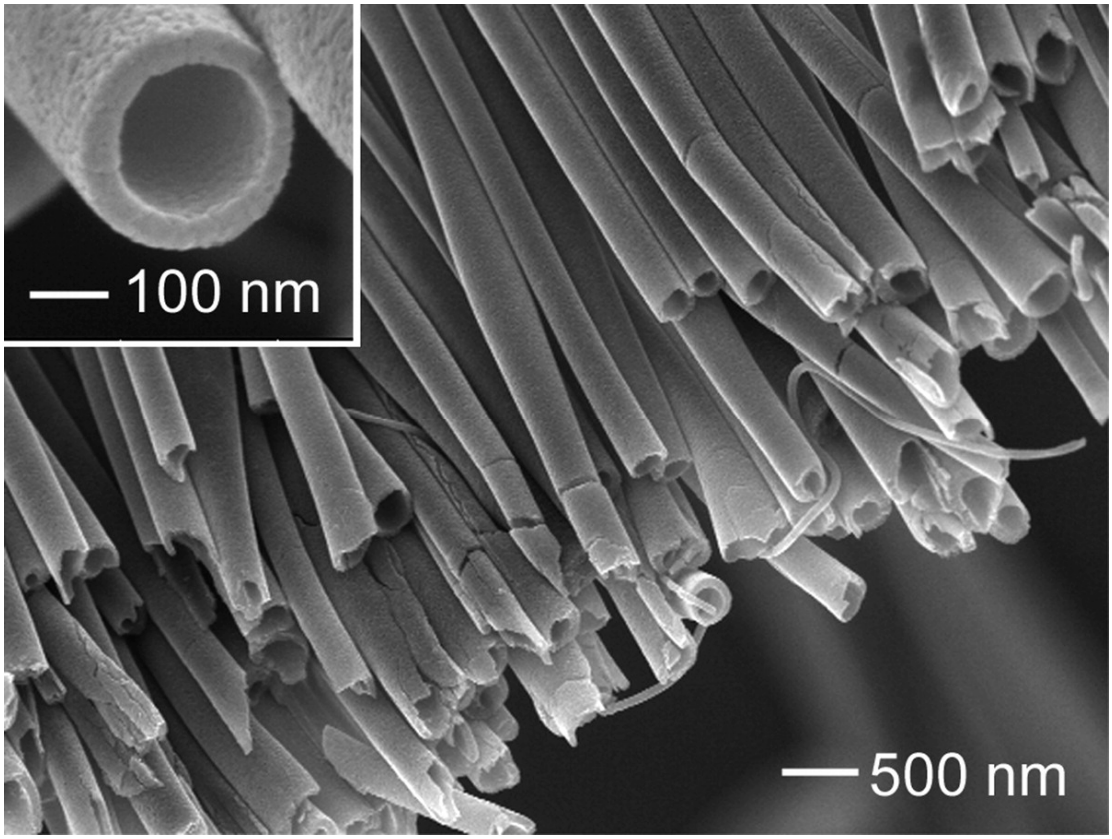

Fig. 7 Representative SEM image of a uniaxially aligned array of titania anatase hollow fibers prepared by electrospinning. Reproduced with permission from Ref [67] © American Chemical Society.

Recently Liu et al.[70] utilized an environmentally friendly molten-salt flux synthesis scheme to prepare high-quality titania nanowires with controllable dimensions. Pulsed laser deposition,[71, 72] protein-mediated,[73] microwave-assisted,[74, 75] and microemulsion[76]

techniques are some other process variations researchers recently explored to synthesis various TNSs.

4. Surface modification of TNSs

Even though, the TNSs are extensively evaluated for various biomedical applications, surface inertness of the material still remains a major challenge in the biomaterials field. To overcome this drawback, various surface modification strategies are being explored by researchers to enhance the favorable interfacial properties for blood-contacting biomedical applications. Furthermore, the development of intelligent drug delivery systems requires precise and controlled release of the therapeutic moiety to minimize the undesired side effects and to maximize the therapeutic activity. Consequently, specific surface chemistries and morphologies are required to enhance the performance of various titania nanostructures for tailoring to drug delivery applications. For example, recently Mandal et al.,[77] using a number of organosilane functionalized titania nanotubes, demonstrated that the release rate of ibuprofen is significantly influenced by the nature of the functional groups on the titania surface. Hydrophobic modifications on the titania surface reduced the drug loading and increased the release kinetics compared to the hydrophilic modified titania nanotubes. Numerous mechanical (e.g.: grinding, polishing, and attrition), chemical (e.g.: chemical modifications, sol-gel methods, and anodic oxidation), and physical methods (e.g.: plasma, thermal spray, ion implantation, and deposition) are commonly used by material scientists to improve the surface properties of TNSs. [78-8586, 87] Representative examples are presented in detail below. However,

additional examples relevant to particular applications can be found in the subsequent biomedical application sections.

Vasilev et al.[88] prepared a tailorable surface functionalized titania nanotube arrays using plasma surface modification followed by target molecule immobilization. Plasma surface modification in presence of allylamine resulted in amine rich surface layer on the titania nanotubes, which facilitated subsequent immobilization of suitable functional moieties to tailor a wide range of biomedical applications. To demonstrate this feasibility, the researchers prepared a layer-by-layer assembly of poly(styrenesulfonate) (PSS) through electrostatic adsorption and poly(ethylene glycol) (PEG) layer through covalent grafting (Fig. 8).

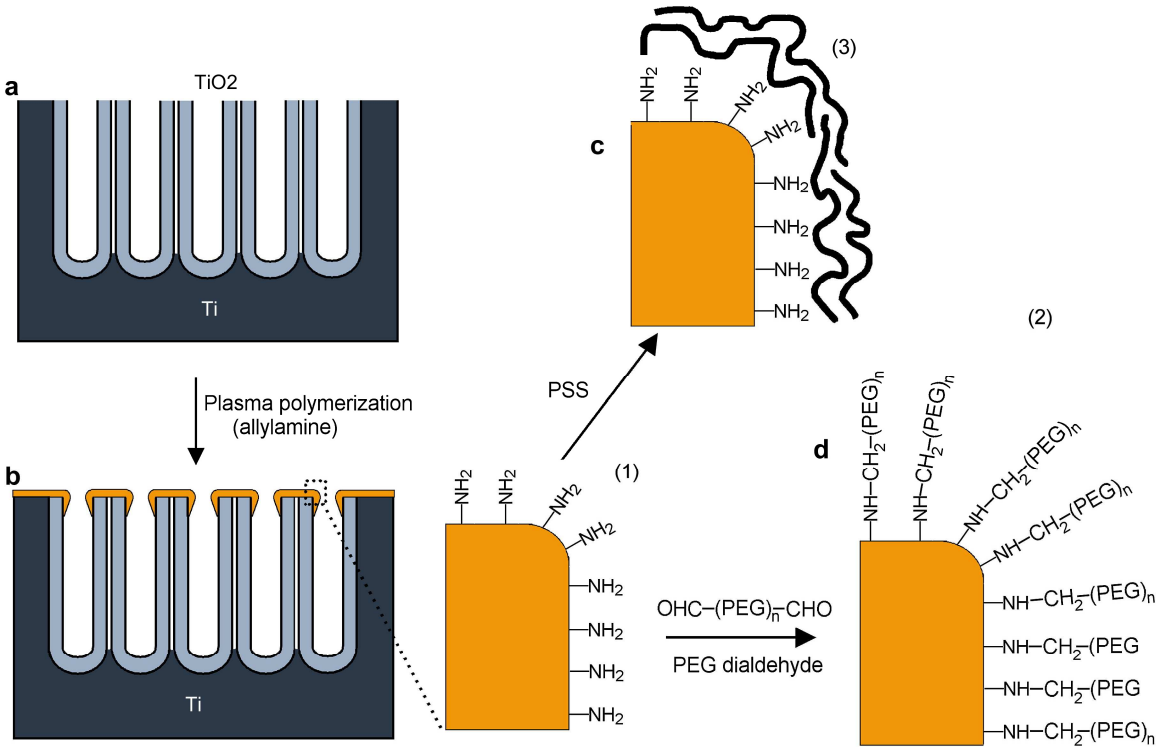

Fig. 8 Scheme for the tailoring of the surface functionalities on TiO_2 nanotube films. Reproduced with permission from Ref [88] © Elsevier.

Neupane et al.[89] prepared titania nanotubes impregnated with gelatin stabilized gold nanoparticles (AuNPs-gelatin) using a simple lyophilization technique, which involves the electrostatic stabilization of the positively charged AuNPs-gelatin particles with the positively charged titania nanotubes. Because of the extremely low cytotoxicity, the AuNPs-gelatin modified titania nanotubes exhibited significantly improved adhesion and propagation of MC3T3-E1 osteoblast cells compared to the bare titania nanotubes. In a similar way, Ma et al.[90] prepared modified titania nanotubes by electrodepositing Ag nanoparticles followed by fibroblast growth factor 2 (FGF-2) immobilization with repeated lyophilization. This modified titania nanotubes showed enhanced human gingival fibroblast (HGF) functions, negligible cytotoxicity, and excellent cytocompatibility compared to the control samples.

Bae et al.[91] explored anodic oxidation to increase the surface roughness of nanotubular titanium implants to provide storage room for the delivery of growth factors to enhance osseointegration. Their study showed that anodic oxidation altered the titania crystal structures through dielectric breakdown that leads to an increase in surface roughness. In another attempt, Vukičević et al.[92] prepared silane modified self-cleaning titania nanorods which can be a potential precursor for developing anti-microbial coatings.

5. Biomedical Applications

5.1 Tissue Engineering

Due to their excellent biocompatibility, low toxicity, good corrosion resistance and favorable mechanical properties including good tensile strength and low density, titanium materials have been used to fabricate many medical implants.[93-99] The success of any clinical implant is dependent on: (a) cell-implant interaction and its effect on the cell proliferation, adhesion, differentiation, migration, and (b) integration of the implant with the surrounding tissue. The aim of this section is to review the current state of the art of the nanostructured titania materials in the field of tissue engineering. Specifically, the effect of titania surface and geometry in-vitro on stem cells and other cell types, and in-vivo on tissues is discussed here.

5.1.1 Nanotopography and Stem cell functionality

Cells naturally exist in a 3D environment known as the extracellular matrix (ECM). This nanosize matrix composed of fibrous proteins (collagen, elastin, fibronectin, fibrillin, laminin) and proteoglycans provides structural and biochemical support to the surrounding cells. For tissue engineering and regeneration, the ECM microenvironment facilitates and guides the stem cells to differentiate and regenerate the tissue without any scar tissue formation.[100] Cell-ECM interaction plays a critical role in cell proliferation, differentiation, adhesion, and migration. In order to mimic the natural ECM, many researchers have tried to create scaffolds with nanoscale features. The matrix elasticity and topography of the ECM mimic substrate can induce and direct the stem cells to differentiate into specific lineages.[101] Mesenchymal stem cells (MSCs) are multipotent stem cells that have the capability of differentiating into variety of cell types: osteoblasts

(bone cells), adipocytes (fat cells), chondrocytes (cartilage cells), endothelial cells, fibroblasts (skin cells), myocytes (muscle cells) and neurons (nerve cells).[102] Yim et al. showed that changes in ECM nanotopography affected the focal adhesion assembly and cytoskeleton organization which in turn affects the differentiation and fate of MSCs.[100] For this reason, several studies have investigated the effect of TiO_2 nanostructures and change in their dimensions on stem cell response and differentiation. It has been previously shown that proliferation, cell spreading and attachment of MSCs on titanium surfaces increased with increase in the roughness of the surface.[103]

Park et al. further exploited the effect of surface topography to cellular responses by reporting that the adhesion, spreading, growth and differentiation of rat bone marrow MSCs was critically dependent on the TiO_2 nanotube dimensions.[104, 105] Vertically oriented TiO_2 nanotubes with diameters between 15 and 100 nm were prepared by anodizing a Ti sheet in a phosphate-fluoride electrolyte at voltages between 1-20 V. They showed that the optimal length scale for cell growth, spreading and differentiation into osteogenic lineage was the smaller diameter nanotubes (≈15 nm) compared to larger diameter nanotubes (≈ 100 nm) where the cells underwent apoptosis. Accelerated focal contact formation that further enhanced cellular activity compared to smooth TiO_2 surfaces was observed on nanotubes smaller than 30 nm. A study comparing the behavior of osteoclasts and osteoblasts on nanotube dimensions also showed that differentiation of hematopoietic stem cells (HSCs) and MSCs into osteoclasts and osteoblasts respectively was stimulated by nanotubes having diameters <30 nm and inhibited by nanotubes having diameters >100nm.[105] A similar nanosize dependence on rat bone marrow MSCs

was seen in ZrO_2 nanotubes and TiO_2 nanotubes coated with AuPd layer. In both the cases, enhanced cellular spreading and differentiation was observed on nanotubes with diameters 15~30 nm, emphasizing that the nanotube size effects dominate over all other possible effects on cell activity.[106] However, cell adhesion was found to be independent of nanotube diameter when these TiO_2 nanotubes were modified to be super-hydrophobic.[107] Wetting behavior and super-hydrophobic nature of these nanotubes enhanced the adsorption of extracellular matrix proteins and showed higher cell attachment after 24 h. Wettability or increase in surface energy was also shown to be the main reason for the increase in cell adhesion by Webster et al. [108]. They showed that Ti and Ti-6Al-4V alloys due to their increased surface area and nanoroughness led to increased osteoblast adhesion.

Contrary results of the cellular response to nanotube dimensions were observed when Oh et al. evaluated the cell adhesion, proliferation, and osteogenic differentiation of human mesenchymal stem cells (hMSCs) on a range of nanotubes with diameters between 30~100 nm.[102, 109, 110] Their TiO_2 nanotubes as shown in Fig. 9, were fabricated by anodization process, heat treated at 500^{o}C for 2 h to transform the amorphous TiO_2 nanotubes into crystallized anatase phase.

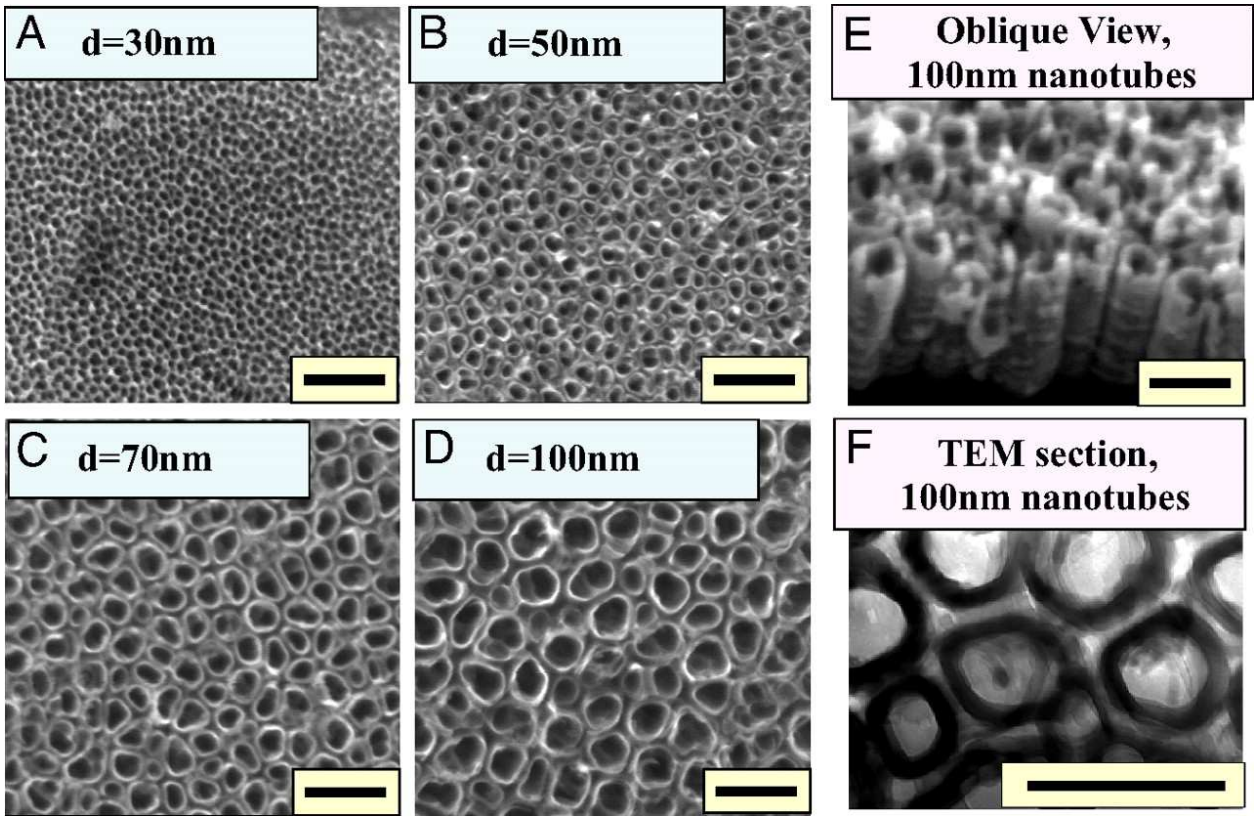

Fig. 9 TiO_2 nanotube. (*A–D*) SEM micrographs (top view) of self-aligned TiO_2 nanotubes with significantly different diameters. The self-assembly layers were generated by anodizing Ti sheets. The images show highly ordered, vertically aligned nanotubes with 4 different nanotube pore diameters, 30, 50, 70, and 100 nm, created by controlling anodizing potentials ranging from 5 to 20 V. (*E*) SEM micrographs (oblique view) of the 100-nm diameter TiO_2 nanotube. (*F*) Cross-sectional transmission electron microscopy (TEM) of the 100-nm diameter TiO_2 nanotubes. (Scale bar, 200 nm.) Reproduced with permission from Ref. [102] © Proceedings of the National Academy of Sciences.

They showed that smaller nanotubes (≈30 nm diameter) promoted cell adhesion and growth with minimal differentiation due to large amounts of protein aggregates attached on the top surface of the nanotubes. On the other hand, higher stem cell elongation and a higher rate of osteogenic differentiation without osteogenic media were observed on larger diameter nanotubes (≈100 nm) due to the induced cytoskeletal stress (Fig. 10).[102] This cytoskeletal stress might be due to the fact that the hMSCs on the large diameter

nanotubes were forced to elongate and stretch to search for protein aggregates that were easily available on the small diameter nanotubes.

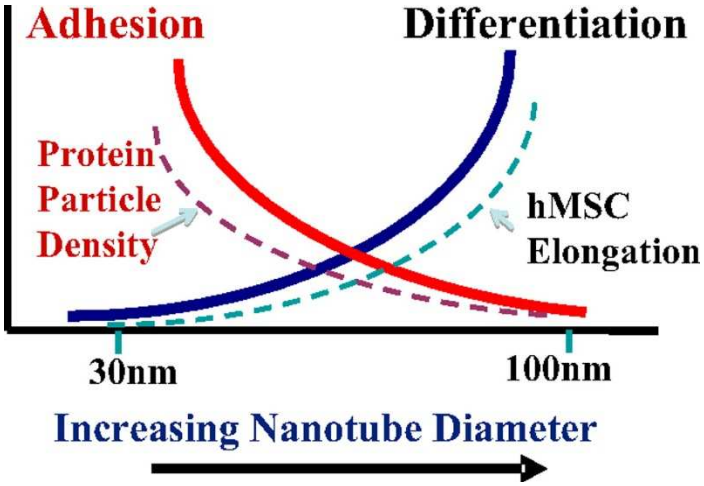

Fig. 10 Schematic illustration of the overall trends of nano cue effects on hMSC fate and morphology after a 24-h culture. The change in hMSC cell adhesion and growth without differentiation (solid red line) has the same trend as protein particle density (broken red line), whereas that of differentiation (solid blue line) has the same trend as hMSC elongation (broken blue line). Reproduced with permission from Ref. [102] © Proceedings of the National Academy of Sciences.

Brammer et al. investigated the role of surface chemistries on stem cell differentiation. They fabricated two kinds of nanotubes: crystalline TiO_2 nanotubes and carbon coated amorphous TiO_2 nanotubes. Both the tubes had similar nanotopographic structure. They found that with respect to the osteoblast adhesion, morphology, and growth, both the tubes behaved in the similar manner. However, higher alkaline phosphatase (ALP), an early marker of bone formation, activity and osteogenic differentiation of hMSCs was observed on carbon-coated TiO_2 nanotubes indicating the effect of surface chemistry on cell functionality.[111] Osteogenic differentiation of MSCs was also explored by Popat et al. [112] where they compared the cell adhesion, proliferation and differentiation of MSCs obtained from male lewis rats on flat Ti surface and crystallized TiO_2 nanotubes.

Anodization technique at 20 V for 20 min followed by annealing at 500^{o}C in dry oxygen ambient was used to fabricate vertically oriented titania nanotubes with a pore size of 80 nm and length of 400 nm. Their results showed 40% increase in the number of cells present on the titania nanotubes compared to the flat Ti surface indicating higher proliferation, cell adhesion and viability on the nanotubular surfaces after 7 days of culture. The MSCs after 7 days of culture had a spreading morphology and appeared to anchor better on the titania nanotubes. After 21 days of culture in the dexamethasone induced media, the MSCs showed 50% increase in the ALP levels and higher amounts of Ca and P on the nanotubes compared to the flat Ti surfaces suggesting that nanotopography plays an important role in stem cell differentiation. Similar results were also obtained with the hierarchical hybrid micropitted titania nanotubes prepared without annealing at 500^{o}C emphasizing the effect of surface nanotopographies on stem cell fate irrespective of their fabrication methods. [113]

Besides the diameter of TiO_2 nanotubes, height of the titania nanopillars and grain size of the Ti substrates also plays a major role in determining the cellular response. Titania nanopillar structures with tunable heights of 15, 55 and 100 nm were fabricated on Ti surfaces using anodization through porous alumina mask. It was shown that on 15 nm high nanopillars, the human skeletal stem cells displayed large focal adhesions, up-regulation of osteogenic transcription factor Runx2 and the expression of osteocalcin and also demonstrated increased levels of certain metabolites (lipoate, sphingosine, and a

variety of amino acids) that are likely to be associated with osteogenic differentiation. [114, 115]

5.1.2 Osteoblast response to nanotopography

For successful osseointegration of an implant *in vivo*, the interaction and adhesion of osteoblasts with the implant surface plays a critical role. Osteoblasts are adult cells in the bone tissue responsible for synthesizing bone and mineralizing the bone matrix[116, 117]. Early studies done by Webster et al. provided the first evidence of enhanced osteoblast adhesion on nanophase alumina and titania compared to conventional ceramics. This was due to the increased nano surface roughness and high surface area of the nanostructures that provided sites for protein adsorption and enhanced the osteoblast adhesion.[108, 118] *In vitro* studies done by Yao et al. also showed that osteoblast adhesions were enhanced on anodized Ti and Ti-6Al-4V alloys compared to conventional unanodized Ti counterparts. Higher adsorption of bone cell adhesion/spreading proteins such as vitronectin and fibronectin, higher ALP activity and higher Ca deposition by osteoblasts was also observed on nanostructured titania.[119, 120]

Accelerated adhesion and proliferation of MC3T3-E1 mouse preosteoblast cells was investigated on the vertically aligned, laterally spaced TiO_2 nanotubes grown on Ti by anodization. These hollow nanotubes were 100 nm in outer diameter and 70 nm in inner diameter with 15 nm wall thickness and 250 nm height.[121, 122] Crystallized anatase structure of TiO_2 nanotubes was obtained after heat treatment at 500^{o}C for 2 h. The adhesion/proliferation of the osteoblasts was significantly accelerated on the TiO_2 nanotubes by 300-400% compared to the Ti surface. SEM micrographs indicate that the

filopodia of propagating osteoblasts goes into the vertical nanopores of the TiO_2 nanotubes (Fig. 11) producing an interlocked cell structure.[122]

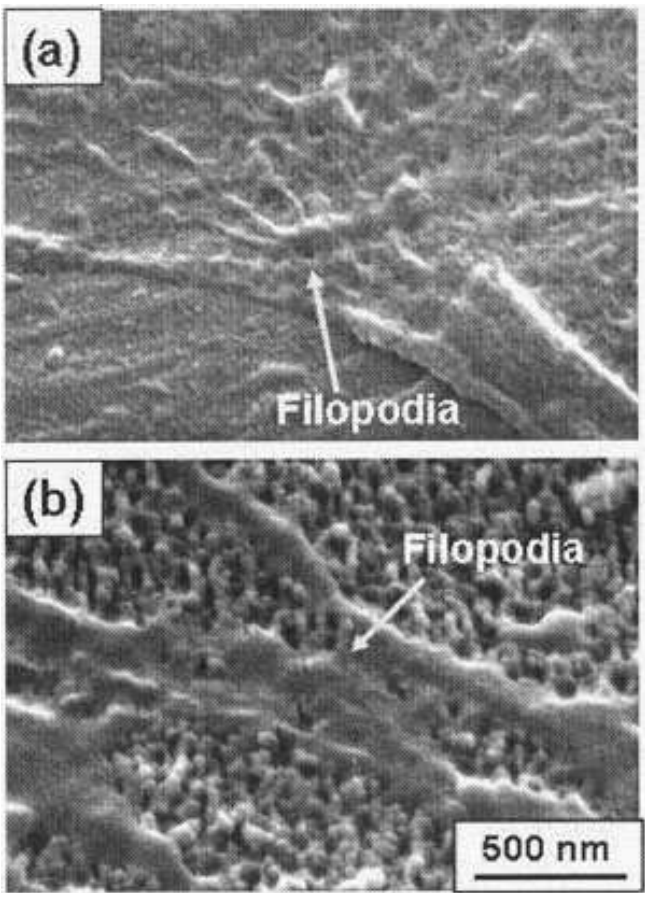

Fig. 11 SEM micrographs showing osteoblast filopodia growth on (a) Ti surface (after 12 h) and (b) TiO2 nanotube surface (after 2 h). Reproduced with permission from Ref. [122] © John Wiley and Sons.

In an attempt to make these TiO_2 nanotubes more bioactive, they were exposed to NaOH solution at 60^{o}C for 60 min, which resulted in the formation of nanofiber like structure (sodium titanate) on top of the nanotubes. *In vitro* hydroxyapatite formation on these nanotubes was accelerated by a factor of 7 as compared to TiO_2 nanotubes without sodium titanate.[121] Such functionality of osteoblasts can vary depending on the pore

diameter of the TiO_2 nanotubes. Brammer et al. showed that increasing nanotube diameters (~ 30 nm to 100 nm) resulted in increased osteoblasts elongation/stretching, increased ALP activity and greater bone forming ability.[123] These findings indicate that TiO_2 nanotubes on the Ti implant surfaces can serve as strong osseointegrating implant interface with optimized cell and bone growth behavior.

Over time, it has been demonstrated that anodized anatase TiO_2 nanotubes are more osteoconductive than conventional Ti surface.[97, 124, 125] Since the crystal structure of the implant surface may affect biological properties, the effect of annealing temperatures of the titania nanotubes on the MC3T3-E1 preosteoblasts was evaluated[93, 126]. A study done by Yu et al. annealed the anodized TiO_2 nanotubes at 450^{o}C, 550^{o}C and 650^{o}C for 3 h in air to acquire different crystalline nanotube phases. The unannealed nanotubes had an amorphous structure that was then converted to anatase structure after annealing at 450^{o}C and to a mixture of rutile and anatase after annealing at 550^{o}C. At 650^{o}C, the nanotubes lost their tubular structure. The proliferation, spreading and mineralization of the preosteoblasts was significantly increased on the anatase-rutile phase followed by the pure anatase phase compared to the amorphous nanotubes and the smooth layers. This indicated that the crystal structure produced by annealing plays a major role in cell proliferation and mineralization *in vitro*.

The cellular functions of osteoblasts can also be influenced by other nanostructured topographies. TiO_2 nanowires (NWs) grown by thermal oxidation on Ti 6 wt% Al-4 wt% V (Ti64) substrates were seeded with human osteocarcoma (HOS) cells.[127] Improved cell

adhesion/proliferation and higher ALP activity were exhibited on the TiO_2 NWs compared to flat TiO_2 and Ti64 substrates. In another study, human osteoblast like MG63 cells were cultured on hydroxyapatite (HA) modified titanate NW scaffolds that were fabricated by a hydrothermal method followed by electrochemical deposition of hydroxyapatite nanoparticles on the NWs.[128] The highly oriented HA layer on the titanate NWs mimic the ECM and promoted enhanced in vitro cell attachment /proliferation and ALP activity indicating the highly osteoconductive nature of these scaffolds.

5.1.3 Chondrocyte response to nanotopography

Chondrocytes, cells found in healthy cartilage, produce and maintain the cartilage matrix. To repair an osteochondral defect, an implant must be an interface between artificial cartilage and native bone. Cultured chondrocytes can create an artificial cartilage and hence are useful for treating cartilage defects. The nanotopographic features of titania have been shown to be promising for repairing bone defects, but these features can also influence chondrocyte behavior and cartilage formation.[129] Savaiano et al. provided the first evidence of chondrocyte response to nanotopographic effects when they showed that nanostructured poly(lactic-co-glycolic acid) (PLGA)/nanophase titania composites can enhance the chondrocyte response compared to surfaces with conventional or micron topographies.[130] Cartilage possesses a nanometer surface roughness and topography due to the presence of proteins. Therefore, the chondrocyte response to the titania nanotopographies is useful in understanding cartilage regeneration. Adhesion of chondrocytes to TiO2 nanotubes was first reported by Burns et al.[131] Human articular chondrocytes were seeded on the anodized amorphous TiO2 nanotubes and observed up

to 21 days. These TiO_2 nanotubes were between 100-200 nm long with 70-80 nm inner diameters. Their results showed enhanced chondrocyte adhesion on the TiO_2 nanotubes compared to the unanodized Ti surface. To further explore the effects of pore size, crystalline anodized TiO_2 nanotubes of four different pore diameters (30, 50, 70 and 100 nm) were fabricated as described previously.[123] SEM micrographs (Fig. 12) showed that the bovine cartilage chondrocyte (BCC cells) that were cultured on these TiO_2 nanotubes produced a dense network of ECM fibrils on the nanotube substrates that were lacking on the flat Ti surface.

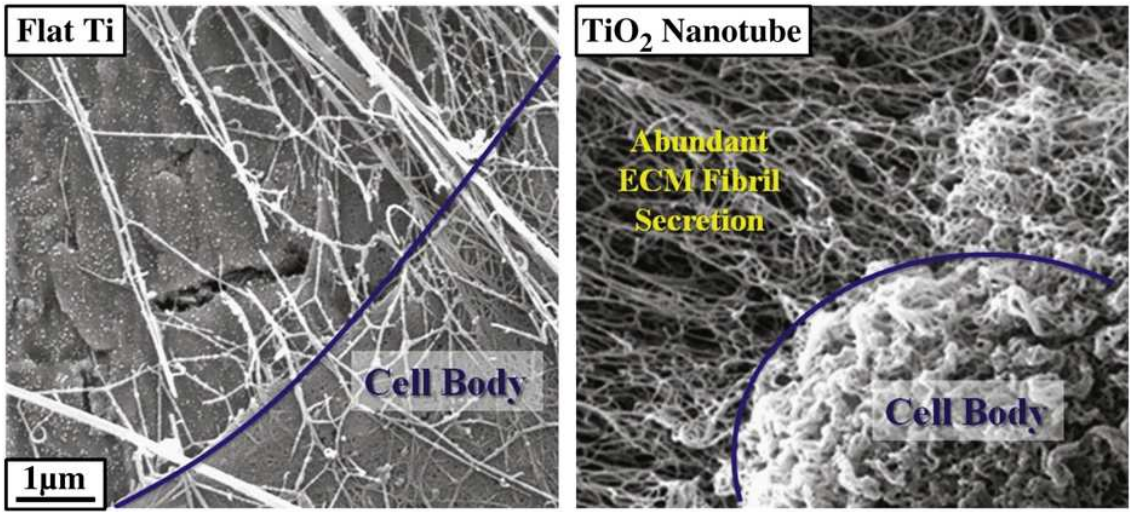

Fig. 12 Higher magnification SEM observations of BCCs reveal a striking difference in the production of extracellular matrix (ECM) fibrils between the flat Ti without a nanostructure vs. TiO2 nanotube surfaces. Fibrils are abundant and extending from all areas of the chondrocyte cell creating a dense network of ECM on the nanotube substrates. Reproduced with permission from Ref. [132] © Elsevier.

BCCs on the nanotubes surface had a characteristic round and spherical chondrocyte morphology where as they appeared to be flattened and spread out on the flat Ti surface (Fig. 13). The authors suggested that the chondrocytes adhered more strongly to the flat Ti surface that led to their spreading compared to the nanotube surface. Chondrocytes are

active cells that produce a large amount of ECM responsible for mechanical properties and joint lubrication. Increased glycosaminoglycan (GAG) secretion and upregulation of aggrecan and collagen II chondrogenic markers were reported on the nanotube substrates, being the highest on the tubes with 70 nm diameter. Therefore, it was concluded that the large diameter was the most promising in cartilage-bone regeneration.[132] A similar chondrocyte response was also reported for TiO_2 nanofibers that were fabricated on Ti-6Al-4V substrate by simple oxidation process as described before.[127] Enhanced BCC adhesion, proliferation, and ECM fibrils production were observed on the TiO_2 NFs compared to the untreated substrates suggesting that chondrocytes have affinity to NFs surface structure.[133]

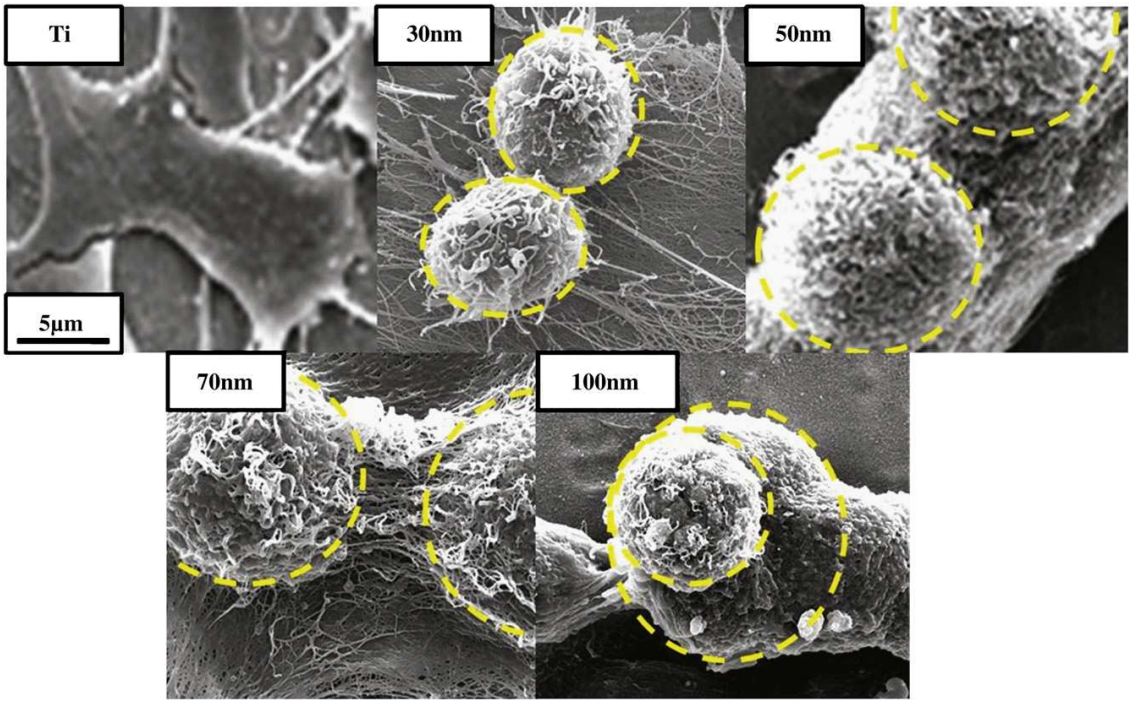

Fig. 13 SEM micrographs of bovine cartilage chondrocytes (BCCs) on flat Ti and 30, 50, 70, and 100 nm diameter TiO_2 nanotube surfaces after 5 days of culture. The yellow dashed lines show the round characteristic shape of the chondrocytes on the nanotube surfaces, which is lacking on the Ti substrate. Reproduced with permission from Ref. [132] © Elsevier.

5.1.4 Endothelial and smooth muscle cell response to nanotopography

Stent thrombosis and restenosis after implantation are major clinical problems associated with vascular prosthetics. Thrombosis is caused by lack of endothelialization or inadequate migration and proliferation of endothelial cells (ECs) over the inner stent wall. Restenosis causes prosthesis narrowing due to the proliferation of vascular smooth muscle cells (VSMCs) that surround the EC layer.[99] After implantation, the stent is in direct contact with the endothelium and EC migration and coverage are responsible for complete endothelialization. Therefore, material used for vascular stent applications should have surface properties that facilitate complete endothelialization, EC migration, proliferation and functioning while reducing the VSMC proliferation.[134] Experiments have shown that anodized TiO_2 nanotubes enhanced the proliferation, functionality, and migration of bovine aortic endothelial cells (BAECs) facilitating ECM deposition and more organized actin cytoskeleton compared to flat Ti surface.[135-137] The TiO_2 nanotube structures also improved the release ratio of nitric oxide (NO)/endothelin-1thereby reducing the platelet aggregation and regulating thrombotic conditions.[137] In addition to the ECs response, Peng et al. also investigated the response of VSMCs by employing mouse aortic vascular smooth muscle cells (MOVAS) on crystalline anodized TiO_2 nanotubes.[135] Nanotubular surfaces showed an increase in EC growth and migration and a decrease in VSMCs proliferation along with an increased secretion of prostaglandin I_2 (PG I_2), an anti-thrombogenic product compared to flat Ti surface. Mohan et al. addressed the problem of late stent restenosis by investigating the proliferation of human umbilical vein endothelial cells (HUVECs) on hydrothermally modified titanium surface.[138, 139] Ti stent prototypes developed using Ti wires were hydrothermally surface

modified to generate nanotopographies on Ti. EC viability was enhanced (>90%) on nanomodified surfaces whereas smooth muscle cell viability was decreased substantially compared to the unmodified Ti surface. NO production was significantly increased, and the platelets also did not adhere to the endothelialized nanostructured Ti.[139] Thrombus deposition studies under static and dynamic conditions were performed using recalcified whole blood. The results showed that unmodified Ti stents had a certain degree of thrombus formation while in the nanomodified stents irrespective of their topography, the thrombus formation was significantly reduced both in static as well as in dynamic conditions (Fig. 14).[138]

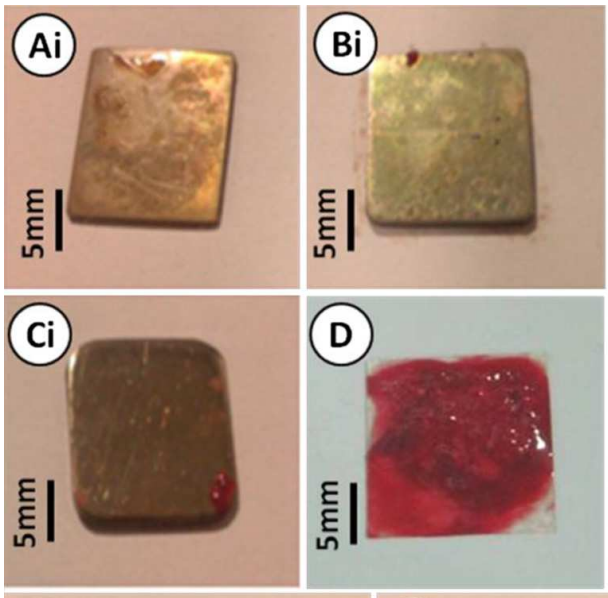

E

Ti samples	Thrombus wt(mg)
NL	56.6 ± 5 **
NP	49.3 ± 3 **
C Ti	76.0 ± 3
PC	92.3 ± 4 aa
Ti stents	**Thrombus wt(mg)**
NL stent	17.1 ± 5 **
NP stent	19.7 ± 1 **
UM stent	33.6 ± 4

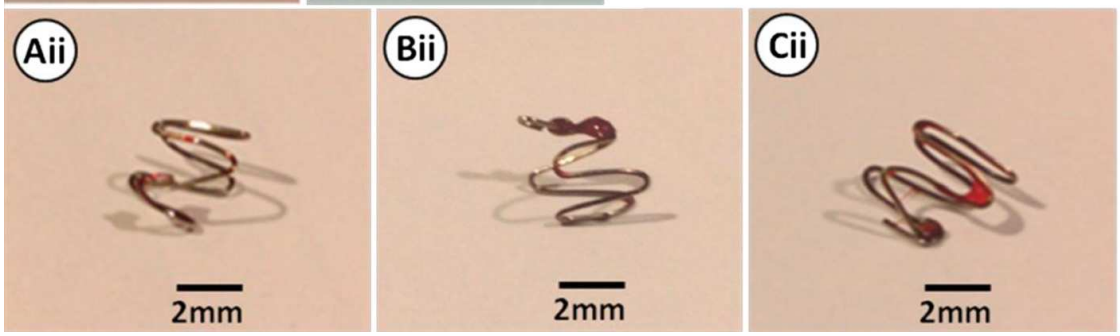

Fig. 14 Thrombus deposition studies on various nanomodified Ti surfaces: (Ai, ii) NL; (Bi, ii) NP; (Ci, ii) C Ti. Top panel (Ai, Bi, Ci) and bottom panel (Aii, Bii, Cii) represent Ti plates and Ti stents exposed to recalcified human blood under static and flow conditions, respectively, showing a reduced thrombus deposition on nanomodified surfaces. (D) Positive control (glass). (E) Table comparing the weight of thrombus deposits on various nanomodified plates and stents with respect to the unmodified samples under static and dynamic flow conditions. $p < 0.01$ implies significantly less thrombus on NL and NP compared with Ti control/UM stent; $p < 0.01$ indicate statistically significant thrombus weight on PC. Reproduced with permission from Ref. [138] © Elsevier.

Zhong et al. further showed that besides the nano cues, chemical stimulus can also affect the ECs response. TiO_2 nanotubes functionalized with polydopamine (PDA) enhanced the ECs elongation, proliferation, and migration and restricted the VSMCs proliferation better than the TiO_2 nanotubes without PDA and flat Ti surface (Fig. 6).[140]

5.1.5 In-vitro inflammatory response of nanostructured titania

Long-term success of an implant in a body depends on complete integration of the implant with the native tissue without causing an inflammatory response. The unwanted inflammatory response induced by macrophages and other defense cells can lead to fibrosis and complete implant rejection. This foreign body response can hinder the natural healing process by comprising the cells involved in tissue regeneration.[141] Titania nanostructures are most promising biomaterials for tissue regeneration since their nanotopography features are on the same nanoscale as the in vivo biomolecules, proteins, enzymes, ECM, etc. that are nanoscale in dimension. Therefore, prior to their application as implantable devices, it is important to understand the effect of nanotopography on the immune response. Ainsile et al. [142] compared the inflammatory response on large diameter (~ 70 nm) titanium nanotubes to flat titanium surface. Compared to the flat Ti

surface, human monocytes cultured on TiO_2 nanotubes had decreased adhesion and irregular morphology with reduced levels of TL-6, IL-10, TNF-α, IL-12 and other inflammatory cytokines. Cytokines proteins produced by immune cells provide signals between immune cells to coordinate the inflammatory response. The rounded morphology and reduced levels of inflammatory cytokines suggested that monocytes on the Ti nanotubes are entering apoptosis. In another study, Smith et al. [141] evaluated the short and long-term immune cell response of titania nanotube arrays compared to flat Ti surface. Whole blood lysates isolated from human blood cultured on titania nanotubes for 2 h, 2 days, and 7 days showed significantly reduced adhesion, proliferation and cytoskeleton organization of monocytes, macrophages, and neutrophils. SEM images (Fig. 15) showed the lack of cell-surface and cell-cell interactions on nanotube surfaces indicating a constrained morphology compared to flat Ti surfaces.

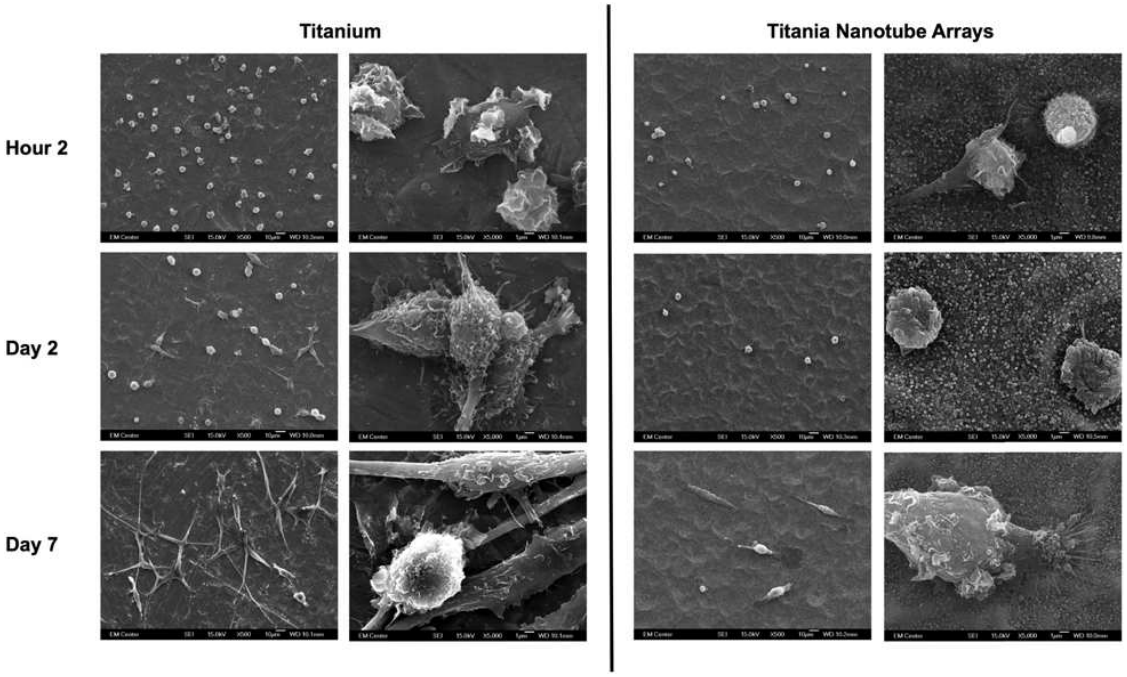

Fig. 15 Representative SEM images of adhered immune cells on Titania nanotube arrays and biomedical grade titanium after 2 hours and 2 and 7 days of incubation in human whole blood lysate. The substrates were coated with a 10 nm layer of gold and imaged at

15 kV. Representative images taken at 500× (left column of both substrate types, scale bar 10 μm) and 5000× (right column of both substrate types, scale bar 1 μm). The images indicate constrained cellular morphology on titania nanotube arrays, while showing increased cell–substrate integration and cell–cell interactions leading to the formation of foreign body giant cells on biomedical grade titanium. Reproduced with permission from Ref. [141] © the Royal Society of Chemistry.

Long term cytokine and chemokine expression (IL-6, IL-8, MIP-1β, and MCP-1) was significantly reduced and amounts of NO increased on the titania nanotubes suggesting their improved biocompatibility. Since cell response is affected by the pore size of nanotubes, Chamberalin et al. [143] explored the inflammatory response of macrophages on crystallized anatase phase TiO_2 nanotubes of different diameters (30, 50, 70 and 100 nm) created by anodization process. It was shown that nanotubes with larger diameter of 70 nm had lower macrophage activation, decreased levels of tumor necrosis factor (TNF) cytokine expression and increased ability to quench free radicals resulting in lower inflammatory response compared to conventional Ti.

5.1.6 Fibroblasts and keratinocytes response to nanotopography

Human dermal fibroblasts (HDF), cells found in the dermis (underlying thick layer of the skin) are responsible for producing ECM and helping the skin to recover from an injury. Human epidermal keratinocytes (HEK) are cells found in the epidermis (outermost layer of the skin) that protect the skin from environmental damage by forming a barrier. Interaction of both HDF and HEK with the implant surface is critical for its long-term success.[47] Smith et al. [47] studied the interaction of HDF and HEK with titania nanotube arrays (70-90 nm diameter, 1-1.5 μm length) that were synthesized by anodization and annealed at 530^{o}C for 3 h to obtain crystallized nanotubes. Cellular adhesion, coverage

and proliferation rate on TiO_2 nanotubes after 4 days of culture was increased in HDF (40% increase) and decreased (90% decreased) in HEK on TiO_2 nanotubes compared to control Ti substrate. Fig. 16 illustrates these results through fluorescent images of HDF and HEK stained by calcein-AM, a cell permanent stain that labels viable cells. They also showed an enhanced cytoskeleton reorganization and membrane protein expression after 4 days of culture in HDF compared to HEK on TiO_2 nanotubes. The authors finally concluded that nanotube arrays provide a favorable template for cellular adhesion and proliferation of HDF inducing fibroblast matrix formation and allowing complete wound healing.

Capellato et al. [144, 145] also utilized HDFs to evaluate the biocompatibility of Ti – 30Ta (Ti with 30 mass % Ta) nanotubes and Ti – 30Ta alloy after 1 and 3 days of culture. Nanotubes were synthesized by anodization in HF (48%) and H_2SO_4 (98%) in 1:9 ratio + 5% DMSO at 35 V for 40 min. The contact angle measurements indicated that the nanotube surface was hydrophilic. Increased fibroblast adhesion, proliferation, elongation and ECM production was observed on the Ti – 30Ta nanotubes compared to the Ti – 30Ta alloy.

Scaffolds functionalized with titania nanotubes (TNTs) were also evaluated for fibroblasts functionality.[146] These TNTs were prepared by hydrothermal method in alkaline medium at 150^{o}C and 4.7 bar ambient pressure and then spin coated on the photopolymerized porous scaffolds. Enhanced fibroblast growth and proliferation was

observed on the scaffolds with TNTs compared to the uncoated scaffolds indicating the importance of nanotopography on cellular response.

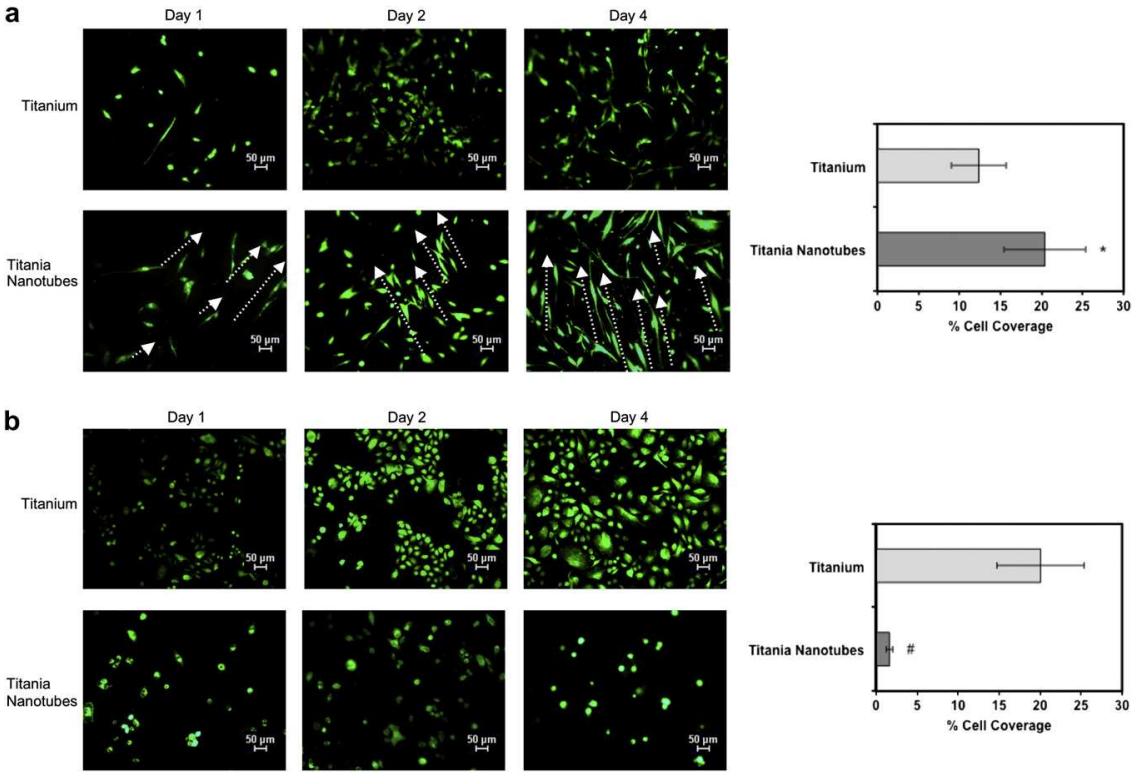

Fig. 16 Representative fluorescence microscopy images (10x magnification) of (a) HDF cells and (b) HEK cells stained with calcein-AM on the control substrate and titania nanotube arrays after 1, 2 and 4 days culture. The results indicate an approximately 40% increase in HDF coverage on titania nanotube arrays compared with the control substrate ($P < 0.05$), and an approximately 92% decrease in HEK coverage on titania nanotube arrays compared with the control substrate ($P < 0.05$). Cellular orientation on titania nanotube arrays is indicated by white arrows. Note that the HEK coverage was calculated using the fluorescence images and Image J software. Experiments were replicated on at least three different samples with at least three different cell populations ($n_{min} = 9$). The error bars in the graph represent the standard deviation. Reproduced with permission from Ref. [47] © Elsevier.

5.1.7 In-vivo response of titania

In vitro cellular response and biocompatibility of the titania implants have been established in numerous studies. However, these implants in-vivo can induce inflammatory responses and fibrosis.[147] Popat et al. [112] investigated the *in vivo*

biocompatibility of titania biomaterials by implanting discs of Ti and TiO_2 nanotubes subcutaneously in male Lewis rat. Histological analysis after 4 weeks showed no fibrous scar tissue was present in the tissues surrounding the Ti implant and was comparable to the healthy tissue. In another study, Smith et al.,[147] looked at the *in vivo* soft tissue response of the TiO_2 nanotubes (100 nm, anodized) and TiO_2 control surfaces. Ti implant disks (5 mm diameter, 2.5 mm thick) were placed in the rat abdominal wall for 1 and 6 weeks. TiO_2 nanotubes showed reduced signal of pro-inflammatory molecule nitric oxide (NO) and a thinner fibrotic capsule at the soft tissue – implant interface. Both the above studies suggested that TiO_2 nanotubes did not cause any adverse foreign body response in vivo.

In vitro, TiO_2 nanotubes have been demonstrated to accelerate osteoblasts adhesion, proliferation, and differentiation.[112, 116, 117, 121-123] *In vivo*, hydroxyapatite (HA) and β-tricalcium phosphate (β-TCP) are the most common clinically used biomaterials. Kubota et al. [148] compared inserts of TiO_2 nanotubes with Ca ions (2 mm diameter, 3 mm thick) to the clinically used HA and β-TCP inserts in a rat femur bone model up to 7 days. TiO_2 nanotubes were observed to be rapidly coated with osteoblasts regenerating new bone matrices. In a more long term study, anodized TiO_2 nanotubes (100 nm, 10 nm wall thickness, 250 nm long) and Ti grit blasted control disks (5 mm diameter, 2.5 mm thick) were implanted in rabbit tibia for 4 weeks. [149] An in vivo mechanical pull-out test showed that the TiO_2 nanotubes improved the in vivo bone bonding strength by nine-folds after 4 weeks of bone growth compared to the Ti grit blasted disks. Histology of the implant (Fig. 17) cross-sections showed a higher bone-implant contact (BIC) area and greater bone formation for the TiO_2 nanotubes compared to the Ti disks.

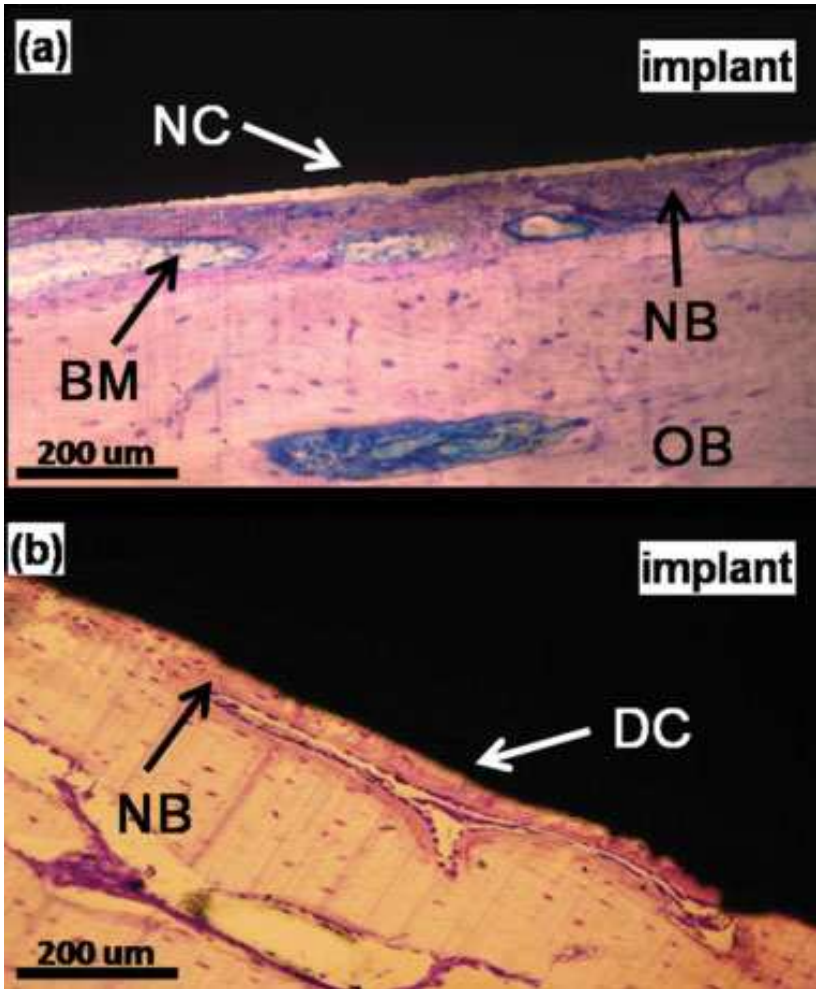

Fig. 17 Hematoxylin and eosin stained ground sections with thickness of 25–50 lm showing direct contact (BC) or non-direct contact (NC) with bone tissue on (a) Ti grit blasted implant and (b) TiO_2 nanotube implant. Bone marrow (BM), old bone (OB), and new bone (NB) are indicated. The no direct contact (NC) area may be an artifact indicating lower adhesive strength or actually be filled with unorganized tissue. Reproduced with permission from Ref. [149] © John Wiley and Sons.

In a similar study, Salou et al. [150] compared the osseointegration of machined (MA), standard alumina grit blasted and acid etched (MICRO) and nanostructured (NANO; TiO_2 nanotubes: anodized, ~30 nm diameter, 160 μm thick) implants in rabbit femurs. The pull-out forces, BIC and the bone growth values after 4 weeks were higher for the

NANO implants compared to other implants indicating that the nano surfaces provides better osseointegration of the bone.

Several studies have evaluated the effect of nanotube diameter on the osseointegration *in vivo* [151-153] for longer periods of time. Wang et al. [151] investigated the effects of anodized TiO_2 nanotubes (anatase; 30 nm, 70 nm, 100 nm) and machined Ti implants (3.3 mm diameter, 8 mm in height) on the gene expression response and bone formation around the implants in mini-pig model. Osterix (OSX), alkaline phosphatase (ALP) and collagen type –I (Col-I) gene expression was upregulated in the TiO_2 nanotubes compared to the machined Ti surface. These transcription factors are expressed by osteoblasts and are vital for osteoblasts differentiation. Tartrate-resistant acid phosphate (TRAP) expressed by osteoclasts was also upregulated in the TiO_2 nanotubes. At all-time points (1, 2, 3, 4 and 5 weeks), the gene expression in the 70 nm diameter TiO_2 nanotubes was the highest indicating that the TiO_2 nanotubes of 70 nm were optimum for osseointegration and osteoconductivity. Histological observations of the bone-implant surface (Fig. 18) at 5 weeks showed the highest degree of bone formation with increase in BIC in 70 nm TiO_2 nanotubes. Similar results of the effects of nanotube diameter on bone formation were also reported in rabbit femur [153] and rat femur [152] model. In both the studies, anodized TiO_2 nanotubes (30-100 nm diameter) were evaluated for BIC, bone volume and removal torque value (indicates degree of osseointegration). In the rat study, highest removal torque values were reported in the 30 nm and 70 nm TiO_2 nanotubes at 2 and 6 weeks respectively. New bone formation expressed by increase in bone area (%) was also reported in the 70 nm TiO_2 nanotubes at the end of 6 weeks. In the rabbit model, higher

bone volume was observed in 30 nm and 70 nm tubes at 4 and 12 weeks respectively. Compared to the control group, 30 nm and 70 nm nanotubes depending on healing time had higher BIC and removal torque value indicating stronger osseointegration and osteogenesis properties. In summary, these findings suggest that different diameters of TiO_2 nanotubes can influence bone formation and osseointegration in-vivo with 70 nm being the optimum diameter for the nanotube implants.

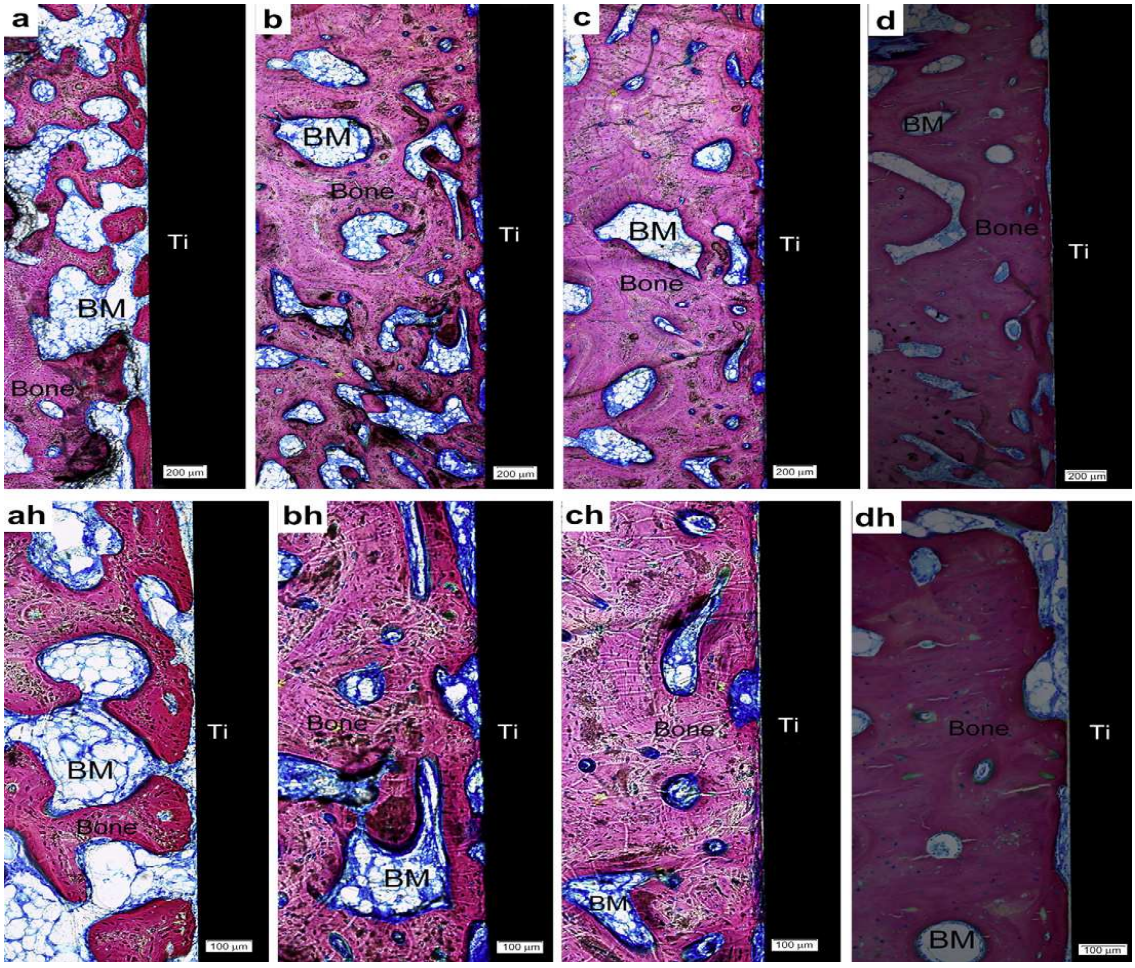

Fig. 18 Digital photographs of stained (methylene blue/basic fuchsine) histological sections at 5 weeks after implantation. Implant in the image is (a) machined, (b) 30 nm TiO_2 nanotubes, (c) 70 nm TiO_2 nanotubes, (d) 100 nm TiO_2 nanotubes. The high magnification of interface between bone and implant is shown in (ah) to (dh) which correspond to machined, 30 nm, 70 nm, 100 nm, respectively. Bone is pink/red, osteoblasts are blue and Ti alloy is black, Ti = titanium, BM = bone marrow. Reproduced with permission from Ref. [151] © Elsevier.

5.2 Drug delivery

Current therapeutic strategies for diseases like cancer, arthritis and others fall short of targeting a specific tissue. Furthermore, systemic circulation of these drugs poses a risk to the patient and has potential to cause many side effects. With the emergence of a plethora of TNSs, the suitability of these surfaces for localized drug delivery has been investigated. The following section will review the use of nanostructured titania materials in the field of drug delivery.

5.2.1. Drug delivery to tissues

Titania nanotubes are extremely small tubes making them an appealing candidate to encapsulate drugs. Titania nanotubes have been extensively researched for clinical applications in orthopedic implants, cardiovascular stents and dentistry to address issues associated with implantation.[154] For example, cardiovascular implants still face many challenges once implanted, such as restenosis and thrombosis. A drug eluting coating on stents or vascular grafts that helps to prevent these issues would be an ideal solution. TiO_2 nanotubes with varying dimensions have been shown to be capable of eluting albumin, as well as sirolimus and paclitaxel, common small molecule drugs used for cardiovascular implants. [155] Furthermore tube height was shown to greatly affect elution kinetics, making TiO_2 nanotubes a good candidate for controlled drug-releasing cardiovascular implant coatings. However, titania nanotubes are extremely versatile in their drug-releasing capabilities. Drug release can target specific tissue and can be controlled in many ways such as modifying nanotube structures, coating nanotubes with a

biopolymer coating, or loading nanotubes with polymeric micelles which act as drug carriers.[156]

Song et al.[157] was able to produce amphiphilic TiO_2 nanotube arrays using a two step anodization procedure with a hydrophobic monolayer modification after the initial step. By utilizing the hydrophobic barrier and the photocatalytic ability of TiO_2, controlled ejection of the hydrophobic barrier leads to a precisely controlled release of a hydrophilic drug (Fig. 19). Titania nanotubes can also be easily dip coated with a polymer in order to create a thin polymer film over the drug-loaded titania nanotubes, allowing for predictable drug release. Gulati et al.[158] showed polymer dip coated titania nanotubes are capable of delivering drugs with predictable release kinetics. Aw et al[159] loaded titania nanotube arrays with drug encapsulated polymeric micelles. By utilizing an external stimulus of ultrasound waves, the drug-loaded nanocarriers were released from the titania nanotubes. The release of the drug can be controlled by parameters on the ultrasonic generator. Further, the stimulated release could be generated and reproduced at anytime within the lifespan on the titania nanotube implant lifespan. In the future, this technique could potentially be used for orthopedic implants or coronary stents. Polymer micelles can also be loaded into the bottom of titania nanotubes with blank micelles on the top in order to delay drug release. This concept was verified with different polymer micelles and also with both water-soluble and water insoluble drugs.[160] Release of the drug carriers can also be stimulated magnetically, when magnetic nanoparticles are loaded at the bottom of the nanotubes. [161] Further, a system for multi- drug delivery systems with sequential release utilizing titania nanotube arrays and polymer micelles as drug carriers

has been created and studied. [162] Drug releasing implants based on titania nanotube arrays for local delivery of therapeutics can potentially address problems such as inflammation, infection and tissue-biomaterial integration. [163]

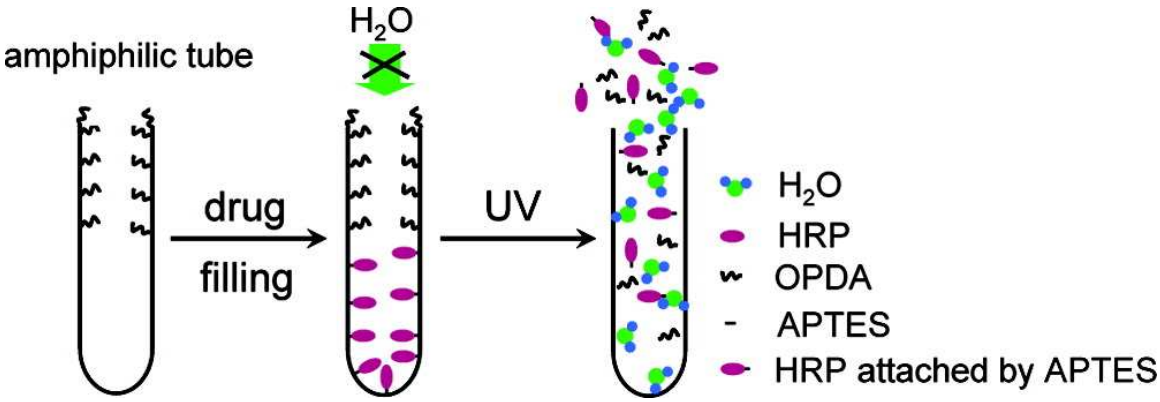

Fig. 19 Representative schematic of how hydrophilic drugs can be released from titania nanotubes by removal of a hydrophobic barrier. Reproduced with permission from Ref. [157] © American Chemical Society.

5.2.2 Cancer drug delivery

Drug release from titania nanostructures has also been shown to be advantageous in cancer treatment. In cancer chemotherapy, cytostatic drugs damage both malignant and normal cells.[164] Therefore, application of nanotechnology and nanomaterials in cancer therapeutics to target specific tissue has attracted much attention in recent years. Doxorubicin, a common cancer medicine, can be easily loaded on TiO_2 nanotubes via adsorption. A study showed that doxorubicin release is pH dependent and TiO_2 nanotubes adsorbed with doxorubicin have the same effect on pancreatic cancer cells as doxorubicin alone, indicating that titania nanotubes could be potential carriers in

antitumor drug controlled-release systems.[165] Titania nanostructures can potentially target specific cancer cells. Lagopati et al.[166] irradiated cultured MCF-7 and MDA-MB-468 breast cancer epithelial cells using UV-A light for 20 min in the presence of sol-gel prepared nanostructured titania aqueous dispersions. The highly malignant MDA-MB-468 cells were induced to undergo apoptotic cell death, while the MCF-7 cells were unimpaired. Shrestha et al. [167] has shown the ability of magnetic TiO_2 nanotubes to photocatalytically kill cancer cells and also photoinduce site-specific release of active molecules such as drugs.

5.2.3 Anti-bacterial drug delivery

Nanostructured titania surfaces have also been investigated for their abilities to prevent bacterial growth (also see section 5.4). Additionally, TNSs are currently being evaluated as a potential platform for various anti-bacterial drug delivery applications. Recently Popat et al. demonstrated that titania nanotubes with 80 nm diameter and 400 nm length loaded with gentamicin were very effective in reducing bacterial adhesion on the surface.[168] Further these titania nanotubes enhanced osteoblast differentiation. A study that compared the ability of various titania nanotubes to release drugs *in vitro* concluded that varying diameters and lengths of the titania nanotubes had a direct impact on gentamicin releasing time.[169] The same surfaces had bactericidal properties against *S. aureus* organism, unlike drug incorporated unmodified titanium. Wang et. al demonstrated that P25 nanoparticles decorated on titania nanotubes improved the loading effect of ibuprofen and a nanotube diameter of 100 nm led to a prolonged and effective

drug release.[170] Huang et al[171] modified titania nanotube surfaces with anti-bacterial drugs for controlled delivery nanosystems. It was shown that controlled release of Enro drugs could be obtained *in vitro* and that the modified titania nanotube surfaces exhibited higher drug availability and longer drug effects *in vivo*. Further, a study reported the controlled release of antimicrobial peptide from a titanium surface consisting of three layers of TiO_2 nanotubes, a thin layer of calcium phosphate coating and a phospholipid film impregnated with the antimicrobial peptide.[172] This surface was effective against both Gram-positive and Gram-negative bacteria.

5.3 Biosensors

TiO_2 can selectively detect the presence of redox species in its vicinity due to its semiconductor property, which becomes highly conductive upon reduction to suboxides, titanium carbide (TiC), or titanium. Taking advantage of this characteristic feature of TiO_2, researchers explored the utility of various TNSs as sensors for high sensitive and quantitative biorecognition of a number of redox proteins, small molecules, and cancer cells.

5.3.1 Detection of glucose and hydrogen peroxide

Xie et al.[173] developed a bioelectrocatalysis system based on titania nanotube electrodes for the quantitative determination of glucose and hydrogen peroxide (H_2O_2). The researchers established a bioelectrocatalytic redox system by embedding glucose oxidases (GOx, EC 1.1.3.4) inside the titania tubular channels and electropolymerizing pyrrole for interfacial immobilization. The amperometric detection mechanism involves

the reduction of glucose catalyzed by GOx with a parallel release of H_2O_2, which results in an electrochemical redox on the titania electrode (Fig. 20). The researchers demonstrated that because of the large surface area-to-volume ratio and stronger micromechanical connection strength, the titanium nanotube arrays showed an enhanced electron transfer capability, good operational reliability, and high response sensitivity compared to the ordinary electrodes. The modified titania electrodes showed a detection limit of 2 x 10^{-3} mM and 2 x 10^{-4} mM for glucose and H_2O_2 respectively.

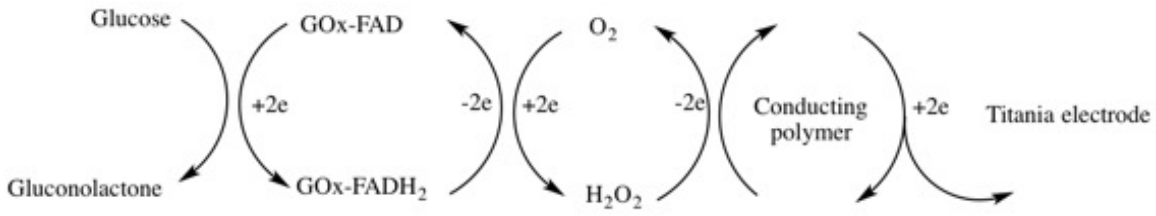

Fig. 20 Schematic illustration of the amperometric detection mechanism of GOx-modified titania biosensor (FAD*: flavin adenine dinucleotide and $FADH_2$: flavin adenine dinucleotide reduced).* Adapted from Ref. [173]

Similar attempts to fabricate titania biosensors by immobilization of GOx was reported by a number of researchers [174-177] and excellent reproducibility, linearity, and a detection limit as low as 2 μM are achieved in most of the cases. Additionally, these biosensors can operate at a very low potential (-0.1V), which will be very beneficial for the selective determination and quantification of glucose in biological samples in the presence of other electrochemically oxidizable interfering species.[175]

In 2006, Viticoli et al.[178] prepared an innovative titania biosensor by co-immobilizing GOx and horseradish peroxidase (HRP) together onto a titania nanostructured surface for the quantitative determination of glucose and H_2O_2. Co-immobilization of the two

enzymes significantly enhanced the electron exchange between the enzymes and electrodes, and resulted in excellent selectivity and fast time response (6-7 seconds) with a very low detection limit of ~1 μM.

Titania biosensors with excellent electron transfer capabilities and electrical conductivities were prepared by Cao et al.[179, 180] by co-immobilization of HRP and thionine chloride (Th) onto highly ordered titania nanotube arrays. In this approach, a drastic increase in the reduction current at about -0.36 V was achieved due to the simultaneous oxidation-reduction of the immobilized HRP-Th moities. Consequently, the biosensor showed a faster electron transfer rate of 1.34 x 10^{-3} cm/s and a response sensitivity of 88.5 μA/mM/L for H_2O_2 sensing. Kafi et al.[181] reported the fabrication of a H_2O_2 biosensor based on co-immobilization of HRP and chitosan onto a Au-modified titania nanotube arrays. The intermediate Au layer significantly enhanced the catalytic activity of HRP and retained its bioactivity. The electrode showed a detection limit of 2 x 10^{-6} mol/L with long linearity and very good reproducibility with a relative standard deviation of 3.75% from 10 successive measurements.

Covalent immobilization of HRP onto a (3-aminopropyl) trimethoxysilane-modified titania nanotubes using 1,4-benzoquinone was explored by Sović et al.[182] for the use in fabrication of H_2O_2 biosensors. Covalent immobilization resulted in high enzyme loading, long term stability, and retained the natural activity of HRP, and demonstrated a detection limit of 35nM H_2O_2. Taking advantage of this high immobilization extent and stability, similar covalent immobilization of GOx and HRP enzyme strategies were

explored by a number of researchers for developing titania based glucose and H_2O_2 biosensors.[183, 184] In addition to GOx and HRP, titania nanotubes immobilized with other biomolecules such cytochrome c,[185-187] hemoglobin (Hb),[188-190] and DNA[191] are also evaluated for glucose and H_2O_2 biosensing applications.

However, even though a remarkable research progress is made in the fabrication of enzyme and other biomolecules based titania biosensors, the activity of these biosensors can be significantly influenced by the relative humidity, pH, temperature, and the presence of denaturing agents.[192] In order to overcome this drawback, enzyme and biomolecule-free titania biosensors modified with platinum, gold and alloys were investigated as suitable alternatives. In one such attempt, Pang et al.[193] prepared a platinum-nanoparticle decorated titania-carbon nanotube arrays (TiO_2/CNT/Pt) which can detect H_2O_2 based on the electrochemical response of the sensor to the oxidation of H_2O_2. The redox current generated at the TiO_2/CNT/Pt electrode showed a linear response with the H_2O_2 concentration with a detection limit of 1 μM (Fig. 21).[193] Utilizing the characteristic photocatalytic self-cleaning property of TiO_2, Song et al.[194] fabricated a self-cleaning non-enzymatic glucose biosensor using Pt-nanoparticle modified titania nanotubes. The researchers successfully demonstrated the reestablishment of the sensor surface before each measurement, facilitated by the self-cleaning properties of TiO_2, to prevent any surface contaminations and drift of the electrode.

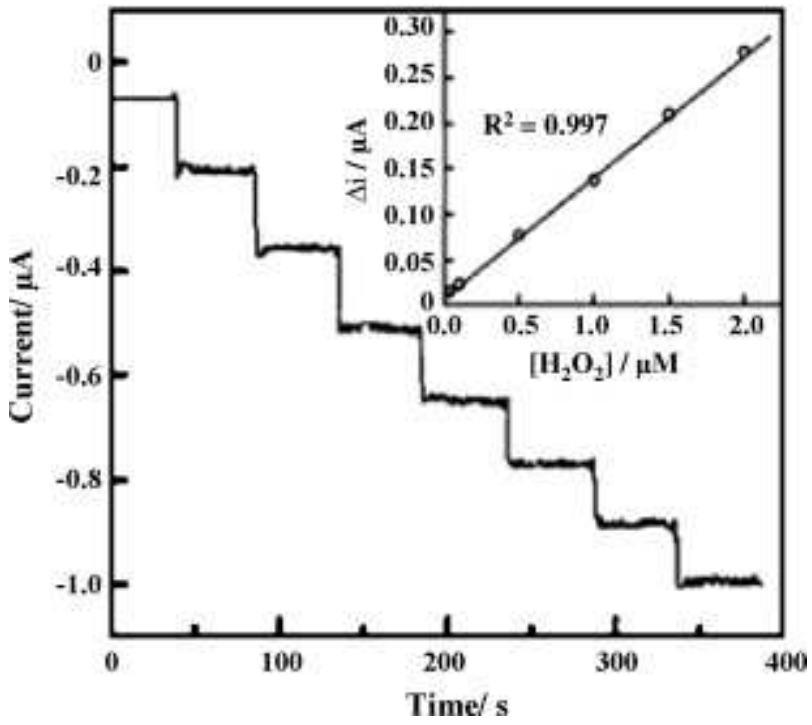

Fig. 21 Ampermetric responses of TiO_2/CNT/Pt electrode to continuously injection of 1 μmol/L H_2O_2 (pH 7.2, 0.067 mol/L PBS). Working potential: 400 mV (vs. Ag/AgCl); the inset shows the calibration curve. Reproduced with permission from Ref [193] © Elsevier.

5.3.2 Detection of biomolecules and biomarkers

Because of the favorable high effective refractive index and analyte sensitivity, titania nanotube arrays are gaining importance in making label-free biosensors for the real-time monitoring of various biomolecules and their interactions. An optical interferometric biosensor based on titania nanotube arrays modified with a protein A capture probe was prepared by Mun et al.[195] for the label-free sensing of rabbit immunoglobulin G (IgG). The titania-biosensors showed exceptional chemical stability in the pH range from 2 to 12 compared to other control sensors made from porous SiO_2 and Al_2O_3. This suggests the suitability for this novel biosensor for applications over a broad range of acidic, basic, and physiological pH conditions. Very recently Solanki et al.[196] reported the fabrication

of a titania-graphene nanocomposite based label-free biosensor functionalized with HRP conjugated antibodies for the specific recognition and detection of *Vibrio cholerae*.

Titania nanotubes modified screen printed carbon electrodes (SPCE), developed by Mandal et al.,[197] provided a cost-effective and robust tool for the selective detection of penicillin binding protein, PBP2a, a marker for *methicillin-resistant Staphylococcus aureus* (*MRSA*). SPCE modification with the titania nanotubes enhanced the electronic properties and effective surface area of the electrode for electrochemical reactions, and consequently increased the sensitivity of detection to concentrations as low as 1-10 ng/μL. An ultrasensitive immunoassay assay for detecting human cardiac troponin I was developed by Kar et al.[198] using titania nanotube arrays modified with carboxyalkylphosphonic acid self-assembled monolayers for the screening of acute myocardial infraction (AMI). Initially, a polyclonal anti-goat troponin antibody was used to capture the cardiac troponin I, followed by conjugating with a secondary antibody anti-mouse fluorescence. Finally, the secondary antibody was conjugated to a fluorophore labeled tertiary antibody for the quantification of troponin 1. The researchers demonstrated an ultralow detection limit of troponin 1 as low as 0.1 pg/mL without any enzymatic amplification, suggesting as a potential point-of-care (POC) biodiagnostic tool for the rapid identification of AMI.

An et al.[199] reported the development of an Au-doped titania nanotube-based low-cost and sensitive photochemical immunosensor for the detection of α-synuclein (α-SYN), as a potential marker for the detection of various human neurodegenerative disorders. In

their approach, antibody AB1 was used to target α-SYN, and GOx was used for signal amplification. The immunosensor showed an excellent reproducibility and stability for determining α-SYN with a detection limit of 34 pg/mL. A rapid and sensitive technique for detecting Listeria monocytogenes was developed by Wang et al.[200] using a monoclonal antibody immobilized titania nanowire immunosensor. The immunosensor showed a selective detection of L. monocytogenes at concentrations as low as 4.7×10^2 cfu/mL within 50 min without any interference from other pathogens.

Because of their strong oxidizing and functionalization properties, various nanostructured titania materials are successfully evaluated as a potential platform for fabricating biosensors for the early screening of different types of cancer. A biocompatible and multi-signal responsive biosensor for the early detection of cancer was developed by Shen et al.[201] based on a titania nanoparticle-carbon nanotube modified electrode. A significantly enhanced electrochemical signal was observed on the electrode covered with the cancer cells compared to the control electrode. Additionally, different electrochemical behavior was also observed in various cancer cells, enabling the particular biorecognition and detection of cancer cells. A titania nanoparticle-based amperometric immunosensor for the rapid determination of α-1-fetoprotein (AFP), an important tumor marker for screening hepatocellular carcinoma and endodermal sinus tumor, was reported by Tan et al.[202]

Zhao et al.[203] recently reported the fabrication a simple p-n heterojunction architecture made from titania nanotubes, a well-known n-type semiconductor, and p-type bismuth

oxyiodide nanoflakes (BiOI NFs). The fabricated BiOI NF/TiO2 NT arrayed p–n junction photoelectrode showed excellent photoresponsibility and superior excitation efficiency due to the unique arrayed structure and the photoelectrochemical synergy effect in the formed p-n junction. Using an immunosandwich protocol with glucose dehydrogenase (GDH) as the enzyme tags, the researchers demonstrated the capability of this novel BiOI NF/TiO2 NT photoelectrode for the accurate detection of vascular endothelial growth factor (VEGF), a very important biomarker for cancer screening. In a similar approach, Cui et al.[204] reported the development of a p-n heterojunction electrode by assembling p-type nickel oxide (NiO) nanoparticles onto n-type surface-coarsened titania nanobelts for detecting the anticancer drug O^6-benzylguanine (O^6BG), lung cancer cells, and the effect of O^6BG on lung cancer cells.

5.4 Antibacterial Applications

Even though the exact mechanism of the antibacterial capability of TiO_2 still a matter of debate, several researchers were tried to explain this biomedically significant feature in a number of ways. In one theory, Sunada et al.[205] proposed that the antibacterial capability of TiO_2 is caused by a photokilling reaction initiated by a partial decomposition of the outer bacterial membrane, followed by disordering of the cytoplasmic membrane, and finally results in the cell death. Using a classical optical hypothesis, Li et al.[206] proposed that the bacterial respiratory proteins can behave as an n-type semiconductor with an approximate band-gap of 2.6-3.1 eV. While in contact with a titania surface, an electron transfer will takes place from the bacteria to TiO_2, which results in a steady loss of

respiratory electrons and ultimately leads to the cell death. To prove their hypothesis, Li et al. fabricated Au-modified titania nanotube arrays and were successfully evaluated for their capabilities for killing *S. aureus* and *E. coli*. This result provides a more convincing support for the classical optical theory, which suggests the disturbance in respiratory electron transfer, than the photokilling effect under darkness within the human body.

Similar to Au-modified TNSs, silver and selenium modified titania nanostructures are also exhibited excellent and long-term antibacterial activity against different bacterial strains including *S. aureus, E. coli, S. epidermidis,* and *P. aeruginosa*.[207-212] In most cases, these materials maintained their antimicrobial activity over 21 – 30 days, suitable for preventing the early-stage to the late-stage bacterial infections.

Although, the titania nanostructures exhibited good antibacterial activity against a variety of pathogenic bacteria, the extent of activity is found to be influenced by the morphology and crystallographic phase of the TNSs. Using Ag-nanoparticle deposited titania nanotubes, Li et al.[213] showed that the anatase nanotubes exhibited the highest activity compared to other crystallographic phases against *E. coli* (Fig. 22A). Additionally, the activities are found to be dependent on the diameter of the nanotubes, however independent of their lengths (Fig. 22B& C).

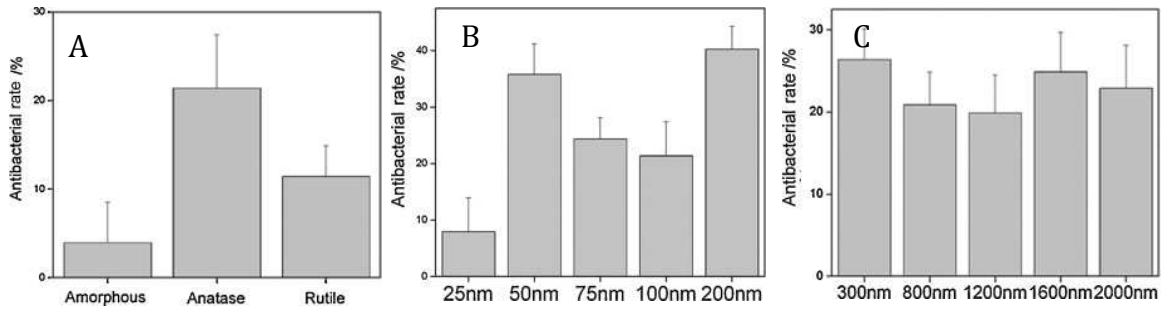

Fig. 22 Influence of morphology and crystallographic phase of the TNSs on the antibacterial efficiency. (A) Antibacterial rates of titania nanatubes with different crystal phases, (B) with different diameters and 800 nm length, and (C) with different lengths and 100 nm diameter. Reproduced with permission from Ref [213] © Elsevier.

6. Conclusion

Titanium and titanium-based alloys have been among the most widely utilized materials for use in implantable biomedical devices since the mid-1900s, when titanium was found to possess tissue-compatible properties. The main factors contributing to the widespread use of titanium in biomedical implants include their impressive mechanical and biocompatible properties, non-toxicity, corrosion resistance, and ease of processability. Titanium reacts naturally with atmospheric oxygen to produce a passive oxide layer on the outside surface, known as titania. This oxide-rich layer creates a hard and scratch-resistant material surface, which protects the metal from environmental factors, improves corrosion and wear resistance. This enables a low coefficient of friction and provides a favorable biocompatible interface for tissue integration. However, the constant exposure of implanted biomaterials to blood and tissue introduces serious and ongoing concerns regarding poor biomaterial integration. Although titanium and titanium-based alloys are among the better choices for implantable biomedical devices, to date, all long-term implanted biomaterials have the potential of initiating physiological events in the form of

inflammation, infection, thrombosis and fibrosis; potentially leading to complete implant rejection. Consequently, improving the proper biointegration is expected to be a primary focus of the future titania research.

Taking advantages of the nanostructured hierarchy of biological structures within the human body, synthetic nanostructured materials can complement, stimulate, and support certain physiological responses with minimal side effects. When the microscale cells interact with their macroscale environment, they do so through countless nanoscale topographical and biochemical cues. In fact, cells are in constant interaction with their surroundings, comprised of nanoscale subcellular structures including fibers, pits, pores and protrusions. Thus, material surfaces with biochemical or topographical modifications similar to that of the natural *in vivo* environment have been shown to elicit cell-specific functionality, enabled through biomimetic cues. In addition, these nanoarchitectures have been shown to promote the activation of signaling pathways that mediate cell adhesion, proliferation and activation, regulate cytokine expression, differentiation, and cellular fusion. Thus, promoting the development of important structural and functional components of healthy tissue-biomaterial integration, preventing infection and biomaterial rejection. These studies point out the benefit of nanoscale architectures on the surface of implantable biomedical devices. Taking advantage of these, various titania nanostructures, such as nanotubes, nanowires, nanorods, nanobelts, and nanoribbons, have been identified as providing a favorable interface for improved cellular functionality. Previous studies have demonstrated improved mesenchymal stem cell functionality, hemocompatibility, osteoblast phenotypic behavior, selective behavioral responses of stem cells and the production of endothelial cell ECM on these

nanostructures. In addition, many of these materials can be filled with various drugs such as antibodies and or growth factors that can be delivered locally to the site of implantation, thus preventing infection and encouraging tissue integration. Titania nanostructures, therefore, are attractive candidate as interfaces for implantable biomedical devices.

As it is clearly evident from this review that, these materials have the potential of being used in a variety of clinical devices including prosthesis, hard and soft tissue grafts, dental and craniofacial implants and cardiovascular stents. The degree of biocompatibility, or the ability of a material to coexist with natural tissue or organs without initiating harm, may therefore be determined by characterizing the extent of a physiological reaction acting to neutralize or sequester the implanted biomedical device from the natural tissue. Overall, these materials demonstrate great potential as next generation biomedical materials. Additionally, much scientific interest has been developed in the recent years to provide a better understanding of the material properties and cellular interactions towards the future innovations in the biomedical science and engineering.

References

1. A. Fujishima and K. Honda, *Nature*, 1972, **238**, 37-38.
2. H. Wang, Z. Guo, S. Wang and W. Liu, *Thin Solid Films*, 2014, **558**, 1-19.
3. C. Jiang and J. Zhang, *J. Mater. Sci. Technol.*, 2013, **29**, 97-122.
4. M. Pelaez, N. T. Nolan, S. C. Pillai, M. K. Seery, P. Falaras, A. G. Kontos, P. S. M. Dunlop, J. W. J. Hamilton, J. A. Byrne, K. O'Shea, M. H. Entezari and D. D. Dionysiou, *Appl. Catal., B: Environmental*, 2012, **125**, 331-349.

5. A. Haring, A. Morris and M. Hu, *Materials*, 2012, **5**, 1890-1909.
6. E. J. Emanuel, *Journal of the American Medical Association*, 2013, **309**, 1589-1590.
7. The U.S. Medical Device Industry in 2012: Challenges at Home and Abroad; http://www.mddionline.com/article/medtech-2012-SWOT; Accessed on Jan 03, 2015.
8. X. Wang, Z. Li, J. Shi and Y. Yu, *Chem. Rev.*, 2014, **114**, 9346-9384.
9. T. Kubo and A. Nakahira, *J. Phys. Chem. C*, 2008, **112**, 1658-1662.
10. V. N. Koparde and P. T. Cummings, *ACS Nano*, 2008, **2**, 1620-1624.
11. J. Sanz, J. Soria, I. Sobrados, S. Yurdakal and V. Augugliaro, *J. Phys. Chem. C*, 2012, **116**, 5110-5115.
12. A. R. Armstrong, G. Armstrong, J. Canales and P. G. Bruce, *Angew. Chem. Int. Ed.*, 2004, **43**, 2286-2288.
13. J. Li, W. Wan, H. Zhou, J. Li and D. Xu, *Chem. Commun.*, 2011, **47**, 3439-3441.
14. R. Giannuzzi, M. Manca, L. De Marco, M. R. Belviso, A. Cannavale, T. Sibillano, C. Giannini, P. D. Cozzoli and G. Gigli, *ACS Appl. Mater. Interfaces*, 2014, **6**, 1933-1943.
15. G. Armstrong, A. R. Armstrong, J. Canales and P. G. Bruce, *Chem. Commun.*, 2005, 2454-2456.
16. C. Bae, H. Yoo, S. Kim, K. Lee, J. Kim, M. M. Sung and H. Shin, *Chem. Mater.*, 2008, **20**, 756-767.
17. D. V. Bavykin, J. M. Friedrich and F. C. Walsh, *Advanced Materials*, 2006, **18**, 2807-2824.
18. A. M. Md Jani, D. Losic and N. H. Voelcker, *Prog. Mater. Sci.*, 2013, **58**, 636-704.
19. A. W. Tan, B. Pingguan-Murphy, R. Ahmad and S. A. Akbar, *Ceramics International*, 2012, **38**, 4421-4435.
20. P. Hoyer, *Langmuir*, 1996, **12**, 1411-1413.
21. T.-S. Kang, A. P. Smith, B. E. Taylor and M. F. Durstock, *Nano Letters*, 2009, **9**, 601-606.
22. C. Bae, Y. Yoon, H. Yoo, D. Han, J. Cho, B. H. Lee, M. M. Sung, M. Lee, J. Kim and H. Shin, *Chem. Mater.*, 2009, **21**, 2574-2576.
23. B. B. Lakshmi, P. K. Dorhout and C. R. Martin, *Chem. Mater.*, 1997, **9**, 857-862.
24. K. Aisu, T. S. Suzuki, E. Nakamura, H. Abe and Y. Suzuki, *J. Ceram. Soc. Jpn.*, 2013, **121**, 915-918.
25. L. Yuan, S. Meng, Y. Zhou and Z. Yue, *J. Mater. Chem. A*, 2013, **1**, 2552-2557.
26. J. Lee, K. S. Hong, K. Shin and J. Y. Jho, *Journal of Industrial and Engineering Chemistry*, 2012, **18**, 19-23.
27. D. Wang, L. Zhang, W. Lee, M. Knez and L. Liu, *Small*, 2013, **9**, 1025-1029.
28. J. H. Kim, X. H. Zhang, J. D. Kim, H. M. Park, S. B. Lee, J. W. Yi and S. I. Jung, *J. Solid State Chem.*, 2012, **196**, 435-440.
29. X. Meng, M. N. Banis, D. Geng, X. Li, Y. Zhang, R. Li, H. Abou-Rachid and X. Sun, *Appl. Surf. Sci.*, 2013, **266**, 132-140.
30. S. Deng, S. W. Verbruggen, Z. He, D. J. Cott, P. M. Vereecken, J. A. Martens, S. Bals, S. Lenaerts and C. Detavernier, *RSC Adv.*, 2014, **4**, 11648-11653.
31. J. Qiu, X. Li, X. Gao, X. Gan, B. Weng, L. Li, Z. Yuan, Z. Shi and Y.-H. Hwang, *J. Mater. Chem.*, 2012, **22**, 23411-23417.

32. K. R. Moonoosawmy, M. Es-Souni, R. Minch, M. Dietze and M. Es-Souni, *CrystEngComm*, 2012, **14**, 474-479.
33. M. Adachi, Y. Murata, M. Harada and S. Yoshikawa, *Chem. Lett.*, 2000, **29**, 942-943.
34. S. Kobayashi, K. Hanabusa, N. Hamasaki, M. Kimura, H. Shirai and S. Shinkai, *Chem. Mater.*, 2000, **12**, 1523-1525.
35. H. Li, Q. Zhou, Y. Gao, X. Gui, L. Yang, M. Du, E. Shi, J. Shi, A. Cao and Y. Fang, *Nano Res.*, 2014, 1-7.
36. G. Gundiah, S. Mukhopadhyay, U. G. Tumkurkar, A. Govindaraj, U. Maitra and C. N. R. Rao, *J. Mater. Chem.*, 2003, **13**, 2118-2122.
37. V. Galstyan, E. Comini, G. Faglia and G. Sberveglieri, *Sensors*, 2013, **13**, 14813-14838.
38. D. V. Bavykin and F. C. Walsh, in *Titanate and Titania Nanotubes: Synthesis*, The Royal Society of Chemistry, 2009, pp. 20-49.
39. L.-k. Tsui and G. Zangari, *J. Electrochem. Soc.*, 2014, **161**, D3066-D3077.
40. S. Rani, S. C. Roy, M. Paulose, O. K. Varghese, G. K. Mor, S. Kim, S. Yoriya, T. J. LaTempa and C. A. Grimes, *Phys. Chem. Chem. Phys.*, 2010, **12**, 2780-2800.
41. J. M. Macak, H. Tsuchiya, A. Ghicov, K. Yasuda, R. Hahn, S. Bauer and P. Schmuki, *Curr. Opin. Solid State Mater. Sci.*, 2007, **11**, 3-18.
42. X. Zhou, N. T. Nguyen, S. Özkan and P. Schmuki, *Electrochem. Commun.*, 2014, **46**, 157-162.
43. D. Gong, C. A. Grimes, O. K. Varghese, W. Hu, R. S. Singh, Z. Chen and E. C. Dickey, *J. Mater. Res.*, 2001, **16**, 3331-3334.
44. V. Galstyan, A. Vomiero, E. Comini, G. Faglia and G. Sberveglieri, *RSC Adv.*, 2011, **1**, 1038-1044.
45. J. M. Macák, H. Tsuchiya and P. Schmuki, *Angew. Chem. Int. Ed.*, 2005, **44**, 2100-2102.
46. B. S. Smith, S. Yoriya, L. Grissom, C. A. Grimes and K. C. Popat, *J. Biomed. Mater. Res., Part A*, 2010, **95A**, 350-360.
47. B. S. Smith, S. Yoriya, T. Johnson and K. C. Popat, *Acta biomater.*, 2011, **7**, 2686-2696.
48. A. L. A. Escada, R. Z. Nakazato and A. P. R. A. Claro, *Nanosci. Nanotechnol. Lett.*, 2013, **5**, 510-512.
49. M. Myahkostupov, M. Zamkov and F. N. Castellano, *Energy Environ. Sci.*, 2011, **4**, 998-1010.
50. J. P. Huang, D. D. Yuan, H. Z. Zhang, Y. L. Cao, G. R. Li, H. X. Yang and X. P. Gao, *RSC Adv.*, 2013, **3**, 12593-12597.
51. K. C. Sun, M. B. Qadir and S. H. Jeong, *RSC Adv.*, 2014, **4**, 23223-23230.
52. S. V. Chong, N. Suresh, J. Xia, N. Al-Salim and H. Idriss, *J. Phys. Chem. C*, 2007, **111**, 10389-10393.
53. H. Li, H. Zhao, Y. Sheng, J. Huang, Y. Song, K. Zheng, Q. Huo and H. Zou, *J Nanopart. Res.*, 2012, **14**, 1-10.
54. T.-Y. Ma, H. Li, T.-Z. Ren and Z.-Y. Yuan, *RSC Adv.*, 2012, **2**, 2790-2796.
55. C. L. Wong, Y. N. Tan and A. R. Mohamed, *J. Environ. Manage.*, 2011, **92**, 1669-1680.
56. H.-H. Ou and S.-L. Lo, *Sep. Purif. Technol.*, 2007, **58**, 179-191.

57. N. Liu, X. Chen, J. Zhang and J. W. Schwank, *Catalysis Today*, 2014, **225**, 34-51.
58. T. Kasuga, M. Hiramatsu, A. Hoson, T. Sekino and K. Niihara, *Langmuir*, 1998, **14**, 3160-3163.
59. T. Kasuga, M. Hiramatsu, A. Hoson, T. Sekino and K. Niihara, *Advanced Materials*, 1999, **11**, 1307-1311.
60. H. Wang, Y. Liu, M. Zhong, H. Xu, H. Huang and H. Shen, *J Nanopart Res*, 2011, **13**, 1855-1863.
61. Y. L. Pang, S. Lim, H. C. Ong and W. T. Chong, *Appl. Catal., A*, 2014, **481**, 127-142.
62. Z.-Y. Yuan and B.-L. Su, *Colloids Surf., A*, 2004, **241**, 173-183.
63. W.-C. Chien, S.-M. Jang and C.-C. Lin, *Advanced Materials Research*, 2011, **148-149**, 1306-1309.
64. B. Ni, F. Li, X. Li, Z. Fu, Y. Zhu and Y. Lu, *Appl. Surf. Sci.*, 2013, **283**, 175-180.
65. P. Liu, H. Zhang, H. Liu, Y. Wang, X. Yao, G. Zhu, S. Zhang and H. Zhao, *J. Am. Chem. Soc.*, 2011, **133**, 19032-19035.
66. C. Wang, X. Zhang, C. Shao, Y. Zhang, J. Yang, P. Sun, X. Liu, H. Liu, Y. Liu, T. Xie and D. Wang, *J. Colloid Interface Sci.*, 2011, **363**, 157-164.
67. D. Li and Y. Xia, *Nano Letters*, 2004, **4**, 933-938.
68. W. Nuansing, S. Ninmuang, W. Jarernboon, S. Maensiri and S. Seraphin, *Materials Science and Engineering: B*, 2006, **131**, 147-155.
69. J.-Y. Chen, H.-C. Chen, J.-N. Lin and C. Kuo, *Mater. Chem. Phys.*, 2008, **107**, 480-487.
70. B. Liu, H. M. Chen, C. Liu, S. C. Andrews, C. Hahn and P. Yang, *J. Am. Chem. Soc.*, 2013, **135**, 9995-9998.
71. A. Bjelajac, V. Djokic, R. Petrovic, G. Socol, I. N. Mihailescu, I. Florea, O. Ersen and D. Janackovic, *Appl. Surf. Sci.*, 2014, **309**, 225-230.
72. J. H. Noh, J. H. Park, H. S. Han, D. H. Kim, B. S. Han, S. Lee, J. Y. Kim, H. S. Jung and K. S. Hong, *J. Phys. Chem. C*, 2012, **116**, 8102-8110.
73. G. Chen, M. Li, F. Li, S. Sun and D. Xia, *Advanced Materials*, 2010, **22**, 1258-1262.
74. C.-C. Chung, T.-W. Chung and T. C. K. Yang, *Ind. Eng. Chem. Res.*, 2008, **47**, 2301-2307.
75. X. Wu, Q.-Z. Jiang, Z.-F. Ma, M. Fu and W.-F. Shangguan, *Solid State Commun.*, 2005, **136**, 513-517.
76. J. Wang, J. Sun and X. Bian, *Materials Science and Engineering: A*, 2004, **379**, 7-10.
77. S. S. Mandal, D. Jose and A. J. Bhattacharyya, *Mater. Chem. Phys.*, 2014, **147**, 247-253.
78. N. Lu, S. Chen, H. Wang, X. Quan and H. Zhao, *J. Solid State Chem.*, 2008, **181**, 2852-2858.
79. W. Zhang, Y. Li, Q. Wang, C. Wang, P. Wang and K. Mao, *Environ Sci Pollut Res*, 2013, **20**, 1431-1440.
80. H. Shi, G. Zhao, M. Liu and Z. Zhu, *Electrochem. Commun.*, 2011, **13**, 1404-1407.
81. S. Sun, W. Yu, Y. Zhang and F. Zhang, *J Mater Sci: Mater Med*, 2013, **24**, 1079-1091.

82. X. Cao, W.-q. Yu, J. Qiu, Y.-f. Zhao, Y.-l. Zhang and F.-q. Zhang, *J Mater Sci: Mater Med*, 2012, **23**, 527-536.
83. L. Zhang, V. M. Menendez-Flores, N. Murakami and T. Ohno, *Appl. Surf. Sci*., 2012, **258**, 5803-5809.
84. S. Farsinezhad, P. R. Waghmare, B. D. Wiltshire, H. Sharma, S. Amiri, S. K. Mitra and K. Shankar, *RSC Adv.*, 2014, **4**, 33587-33598.
85. S. Kim, M. Kim, S.-H. Hwang and S. K. Lim, *Appl. Catal., B*, 2012, **123–124**, 391-397.
86. M. Kulkarni, A. Mazare, P. Schmuki and A. Iglic, in *Nanomedicine*, eds. A. Seifalian, A. de Mel and D. Kalaskar, One Central Press, 2014, pp. 111-136.
87. X. Liu, P. K. Chu and C. Ding, *Materials Science and Engineering: R: Reports*, 2004, **47**, 49-121.
88. K. Vasilev, Z. Poh, K. Kant, J. Chan, A. Michelmore and D. Losic, *Biomaterials*, 2010, **31**, 532-540.
89. M. P. Neupane, I. S. Park, T. S. Bae, H. K. Yi, M. Uo, F. Watari and M. H. Lee, *J. Mater. Chem*., 2011, **21**, 12078-12082.
90. Q. Ma, S. Mei, K. Ji, Y. Zhang and P. K. Chu, *J. Biomed. Mater. Res., Part A*, 2011, **98A**, 274-286.
91. I.-H. Bae, K.-D. Yun, H.-S. Kim, B.-C. Jeong, H.-P. Lim, S.-W. Park, K.-M. Lee, Y.-C. Lim, K.-K. Lee, Y. Yang and J.-T. Koh, *J. Biomed. Mater. Res., Part B*, 2010, **93B**, 484-491.
92. U. Vukicevic, S. Ziemian, A. Bismarck and M. S. P. Shaffer, *J. Mater. Chem*., 2008, **18**, 3448-3453.
93. W. Yu, Y. Zhang, X. Jiang and F. Zhang, *Oral diseases*, 2010, **16**, 624-630.
94. H. Kim, S.-H. Choi, J.-J. Ryu, S.-Y. Koh, J.-H. Park and I.-S. Lee, *Biomedical Materials*, 2008, **3**, 025011.
95. Z. Chen, Y. Takao, W. Wang, T. Matsubara and L. Ren, *Biomedical Materials*, 2009, **4**, 065003.
96. W.-q. Yu, J. Qiu, L. Xu and F.-q. Zhang, *Biomedical Materials*, 2009, **4**, 065012.
97. K. Das, S. Bose and A. Bandyopadhyay, *J. Biomed. Mater. Res., Part A*, 2009, **90**, 225-237.
98. G. Chen, Z. Wang, H. Bai, J. Li and H. Cai, *Biomedical materials*, 2009, **4**, 015017.
99. S. Wu, Z. Weng, X. Liu, K. Yeung and P. Chu, *Adv. Funct. Mater*., 2014, **24**, 5464-5481.
100. E. K. Yim, E. M. Darling, K. Kulangara, F. Guilak and K. W. Leong, *Biomaterials*, 2010, **31**, 1299-1306.
101. A. Pittrof, J. Park, S. Bauer and P. Schmuki, *Acta Biomater*., 2012, **8**, 2639-2647.
102. S. Oh, K. S. Brammer, Y. J. Li, D. Teng, A. J. Engler, S. Chien and S. Jin, *Proc. Natl. Acad. Sci. U. S. A*., 2009, **106**, 2130-2135.
103. D. S. Kommireddy, S. M. Sriram, Y. M. Lvov and D. K. Mills, *Biomaterials*, 2006, **27**, 4296-4303.
104. J. Park, S. Bauer, K. von der Mark and P. Schmuki, *Nano letters*, 2007, **7**, 1686-1691.

105. J. Park, S. Bauer, K. A. Schlegel, F. W. Neukam, K. von der Mark and P. Schmuki, *Small*, 2009, **5**, 666-671.
106. S. Bauer, J. Park, J. Faltenbacher, S. Berger, K. von der Mark and P. Schmuki, *Integr. Biol.*, 2009, **1**, 525-532.
107. S. Bauer, J. Park, K. v. d. Mark and P. Schmuki, *Acta Biomater.*, 2008, **4**, 1576-1582.
108. T. J. Webster and J. U. Ejiofor, *Biomaterials*, 2004, **25**, 4731-4739.
109. S. Oh, K. S. Brammer, Y. J. Li, D. Teng, A. J. Engler, S. Chien and S. Jin, *Proc. Natl. Acad. Sci. U. S. A.*, 2009, **106**, E61-E61.
110. K. S. Brammer, S. Oh, C. J. Frandsen and S. Jin, *JOM*, 2010, **62**, 50-55.
111. K. S. Brammer, C. Choi, C. J. Frandsen, S. Oh, G. Johnston and S. Jin, *Acta Biomater.*, 2011, **7**, 2697-2703.
112. K. C. Popat, L. Leoni, C. A. Grimes and T. A. Desai, *Biomaterials*, 2007, **28**, 3188-3197.
113. L. Zhao, S. Mei, P. K. Chu, Y. Zhang and Z. Wu, *Biomaterials*, 2010, **31**, 5072-5082.
114. L. E. McNamara, T. Sjöström, K. E. Burgess, J. J. Kim, E. Liu, S. Gordonov, P. V. Moghe, R. Meek, R. O. Oreffo and B. Su, *Biomaterials*, 2011, **32**, 7403-7410.
115. T. Sjöström, M. J. Dalby, A. Hart, R. Tare, R. O. Oreffo and B. Su, *Acta Biomater.*, 2009, **5**, 1433-1441.
116. K. S. Brammer, S. Oh, C. J. Frandsen and S. Jin, *Biomater Sci Eng. InTech*, 2011, 193-210.
117. K. S. Brammer, C. J. Frandsen and S. Jin, *Trends Biotechnol.*, 2012, **30**, 315-322.
118. T. J. Webster, R. W. Siegel and R. Bizios, *Biomaterials*, 1999, **20**, 1221-1227.
119. C. Yao, V. Perla, J. L. McKenzie, E. B. Slamovich and T. J. Webster, *J. Biomed. Nanotechnol.*, 2005, **1**, 68-73.
120. N. G. Durmus and T. J. Webster, *Nanomedicine*, 2012, **7**, 791-793.
121. S. Oh and S. Jin, *Materials Science and Engineering: C*, 2006, **26**, 1301-1306.
122. S. Oh, C. Daraio, L. H. Chen, T. R. Pisanic, R. R. Finones and S. Jin, *J. Biomed. Mater. Res., Part A*, 2006, **78**, 97-103.
123. K. S. Brammer, S. Oh, C. J. Cobb, L. M. Bjursten, H. v. d. Heyde and S. Jin, *Acta Biomater.*, 2009, **5**, 3215-3223.
124. W. q. Yu, X. q. Jiang, F. q. Zhang and L. Xu, *J. Biomed. Mater. Res., Part A*, 2010, **94**, 1012-1022.
125. J. He, W. Zhou, X. Zhou, X. Zhong, X. Zhang, P. Wan, B. Zhu and W. Chen, *J Mater Sci: Mater Med*, 2008, **19**, 3465-3472.
126. Y. Bai, I. S. Park, H. H. Park, M. H. Lee, T. S. Bae, W. Duncan and M. Swain, *Surf. Interface Anal.*, 2011, **43**, 998-1005.
127. B. Dinan, D. Gallego-Perez, H. Lee, D. Hansford and S. Akbar, *Ceram. Int.*, 2013, **39**, 5949-5954.
128. H. Zhao, W. Dong, Y. Zheng, A. Liu, J. Yao, C. Li, W. Tang, B. Chen, G. Wang and Z. Shi, *Biomaterials*, 2011, **32**, 5837-5846.
129. K. Popat, *Nanotechnology in Tissue Engineering and Regenerative Medicine*, CRC Press, 2010.
130. J. K. Savaiano and T. J. Webster, *Biomaterials*, 2004, **25**, 1205-1213.

131. K. Burns, C. Yao and T. J. Webster, *J. Biomed. Mater. Res., Part A*, 2009, **88**, 561-568.
132. K. S. Brammer, S. Oh, C. J. Frandsen, S. Varghese and S. Jin, *Materials Science and Engineering: C*, 2010, **30**, 518-525.
133. A. Tan, A. Dalilottojari, B. Pingguan-Murphy, R. Ahmad and S. Akbar, *Ceram. Int.*, 2014, **40**, 8301-8304.
134. J. Ako, H. N. Bonneau, Y. Honda and P. J. Fitzgerald, *Am. J. Cardiol.*, 2007, **100**, S3-S9.
135. L. Peng, M. L. Eltgroth, T. J. LaTempa, C. A. Grimes and T. A. Desai, *Biomaterials*, 2009, **30**, 1268-1272.
136. J. Park, S. Bauer, P. Schmuki and K. von der Mark, *Nano letters*, 2009, **9**, 3157-3164.
137. K. S. Brammer, S. Oh, J. O. Gallagher and S. Jin, *Nano letters*, 2008, **8**, 786-793.
138. C. Mohan, K. Chennazhi and D. Menon, *Acta Biomater.*, 2013, **9**, 9568-9577.
139. C. C. Mohan, P. Sreerekha, V. Divyarani, S. Nair, K. Chennazhi and D. Menon, *J. Mater. Chem.*, 2012, **22**, 1326-1340.
140. S. Zhong, R. Luo, X. Wang, L. Tang, J. Wu, J. Wang, R. Huang, H. Sun and N. Huang, *Colloids Surf., B*, 2014, **116**, 553-560.
141. B. S. Smith, P. Capellato, S. Kelley, M. Gonzalez-Juarrero and K. C. Popat, *Biomater. Sci.*, 2013, **1**, 322-332.
142. K. M. Ainslie, S. L. Tao, K. C. Popat, H. Daniels, V. Hardev, C. A. Grimes and T. A. Desai, *J. Biomed. Mater. Res., Part A*, 2009, **91**, 647-655.
143. L. M. Chamberlain, K. S. Brammer, G. W. Johnston, S. Chien and S. Jin, *J. Biomater. Nanobiotechnol.,* 2011, **2**, 293-300.
144. P. Capellatoa, B. S. Smith, K. C. Popat and A. P. R. Alves Claroa, *Materials Science and Engineering: C*, 2012, **32**, 2060-2067.
145. P. Capellato, B. S. Smith, K. C. Popat and A. P. Alves Claro, Materials Science Forum, 2015.
146. S. Beke, R. Barenghi, B. Farkas, I. Romano, L. Kőrösi, S. Scaglione and F. Brandi, *Materials Science and Engineering: C*, 2014, **44**, 38-43.
147. G. C. Smith, L. Chamberlain, L. Faxius, G. W. Johnston, S. Jin and L. M. Bjursten, *Acta Biomater.*, 2011, **7**, 3209-3215.
148. S. Kubota, K. Johkura, K. Asanuma, Y. Okouchi, N. Ogiwara, K. Sasaki and T. Kasuga, *J Mater Sci: Mater Med*, 2004, **15**, 1031-1035.
149. L. M. Bjursten, L. Rasmusson, S. Oh, G. C. Smith, K. S. Brammer and S. Jin, *J. Biomed. Mater. Res., Part A*, 2010, **92**, 1218-1224.
150. L. Salou, A. Hoornaert, G. Louarn and P. Layrolle, *Acta Biomater.*, 2015, **11**, 494-502.
151. N. Wang, H. Li, W. Lü, J. Li, J. Wang, Z. Zhang and Y. Liu, *Biomaterials*, 2011, **32**, 6900-6911.
152. Y.-A. Yi, Y.-B. Park, H. Choi, K.-W. Lee, S.-J. Kim, K.-M. Kim, S. Oh and J.-S. Shim, *Journal of Nanomaterials*, 2015, DOI: 10.1155/2015/581713.
153. C.-G. Kang, Y.-B. Park, H. Choi, S. Oh, K.-W. Lee, S.-H. Choi and J.-S. Shim, *Journal of Nanomaterials*.
154. D. Losic, M. S. Aw, A. Santos, K. Gulati and M. Bariana, *Expert Opin. Drug Delivery*, 2015, **12**, 103-127.

155. L. Peng, A. D. Mendelsohn, T. J. LaTempa, S. Yoriya, C. A. Grimes and T. A. Desai, *Nano Letters*, 2009, **9**, 1932-1936.
156. M. Sinn Aw, M. Kurian and D. Losic, *Biomater. Sci.*, 2014, **2**, 10-34.
157. Y.-Y. Song, F. Schmidt-Stein, S. Bauer and P. Schmuki, *J. Am. Chem. Soc.*, 2009, **131**, 4230-4232.
158. K. Gulati, S. Ramakrishnan, M. S. Aw, G. J. Atkins, D. M. Findlay and D. Losic, *Acta Biomater.*, 2012, **8**, 449-456.
159. M. S. Aw and D. Losic, *Int. J. Pharm.*, 2013, **443**, 154-162.
160. M. Sinn Aw, J. Addai-Mensah and D. Losic, *Macromol. Biosci.*, 2012, **12**, 1048-1052.
161. M. S. Aw, J. Addai-Mensah and D. Losic, *J. Mater. Chem.*, 2012, **22**, 6561-6563.
162. M. S. Aw, J. Addai-Mensah and D. Losic, *Chemical Communications*, 2012, **48**, 3348-3350.
163. K. Gulati, M. S. Aw, D. Findlay and D. Losic, *Ther. Delivery*, 2012, **3**, 857-873.
164. S. K. Sahoo and V. Labhasetwar, *Drug discovery today*, 2003, **8**, 1112-1120.
165. Y. Wang, L. Yuan, C. Yao, J. Fang and M. Wu, *J. Nanosci. Nanotechnol.*, 2015, **15**, 4143-4148.
166. N. Lagopati, P. V. Kitsiou, A. I. Kontos, P. Venieratos, E. Kotsopoulou, A. G. Kontos, D. D. Dionysiou, S. Pispas, E. C. Tsilibary and P. Falaras, *J. Photochem. Photobiol., A*, 2010, **214**, 215-223.
167. N. K. Shrestha, J. M. Macak, F. Schmidt-Stein, R. Hahn, C. T. Mierke, B. Fabry and P. Schmuki, *Angew. Chem., Int. Ed. Engl.*, 2009, **48**, 969-972.
168. K. C. Popat, M. Eltgroth, T. J. LaTempa, C. A. Grimes and T. A. Desai, *Biomaterials*, 2007, **28**, 4880-4888.
169. N. Çalışkan, C. Bayram, E. Erdal, Z. Karahaliloğlu and E. B. Denkbaş, *Materials Science and Engineering: C*, 2014, **35**, 100-105.
170. Z. Wang, C. Xie, F. Luo, P. Li and X. Xiao, *Appl. Surf. Sci.*, 2015, **324**, 621-626.
171. P. Huang, J. Wang, S. Lai, F. Liu, N. Ni, Q. Cao, W. Liu, D. Y. B. Deng and W. Zhou, *J. Mater. Chem. B*, 2014, **2**, 8616-8625.
172. M. Kazemzadeh-Narbat, B. F. L. Lai, C. Ding, J. N. Kizhakkedathu, R. E. W. Hancock and R. Wang, *Biomaterials*, 2013, **34**, 5969-5977.
173. Y. Xie, L. Zhou and H. Huang, *Biosens. Bioelectron.*, 2007, **22**, 2812-2818.
174. W. Wang, Y. Xie, Y. Wang, H. Du, C. Xia and F. Tian, *Mikrochim Acta*, 2014, **181**, 381-387.
175. P. Benvenuto, A. K. M. Kafi and A. Chen, *J. Electroanal. Chem.*, 2009, **627**, 76-81.
176. H. Cao, Y. Zhu, L. Tang, X. Yang and C. Li, *Electroanalysis*, 2008, **20**, 2223-2228.
177. H.-C. Lee, L.-F. Zhang, J.-L. Lin, Y.-L. Chin and T.-P. Sun, *Sensors*, 2013, **13**, 14161-14174.
178. M. Viticoli, A. Curulli, A. Cusma, S. Kaciulis, S. Nunziante, L. Pandolfi, F. Valentini and G. Padeletti, *Materials Science and Engineering: C*, 2006, **26**, 947-951.
179. Y. Zhang, P. Xiao, X. Zhou, D. Liu, B. B. Garcia and G. Cao, *J. Mater. Chem.*, 2009, **19**, 948-953.
180. P. Xiao, Y. Zhang and G. Cao, *Sens. Actuators, B*, 2011, **155**, 159-164.

181. A. K. M. Kafi, G. Wu and A. Chen, *Biosens. Bioelectron.*, 2008, **24**, 566-571.
182. D. Sović, A. Gajović and D. Iveković, *Electrochimica Acta*, 2011, **56**, 9953-9960.
183. Y. Xie and Y. Zhao, *Materials Science and Engineering: C*, 2013, **33**, 5028-5035.
184. Z. Zhang, Y. Xie, Z. Liu, F. Rong, Y. Wang and D. Fu, *J. Electroanal. Chem.*, 2011, **650**, 241-247.
185. Y. Astuti, E. Topoglidis, A. G. Cass and J. R. Durrant, *Anal. Chim. Acta*, 2009, **648**, 2-6.
186. A. Zhu, Y. Luo and Y. Tian, *Analytical Chemistry*, 2009, **81**, 7243-7247.
187. G. Zhao, Y. Lei, Y. Zhang, H. Li and M. Liu, *J. Phys. Chem. C*, 2008, **112**, 14786-14795.
188. X. Xiao, W. Lu and X. Yao, *Electroanalysis*, 2008, **20**, 2247-2252.
189. M. Liu, G. Zhao, K. Zhao, X. Tong and Y. Tang, *Electrochem. Commun.*, 2009, **11**, 1397-1400.
190. A. K. M. Kafi, G. Wu, P. Benvenuto and A. Chen, *J. Electroanal. Chem.*, 2011, **662**, 64-69.
191. P.-H. Lo, S. A. Kumar and S.-M. Chen, *Colloids Surf., B*, 2008, **66**, 266-273.
192. R. Wilson and A. P. F. Turner, *Biosens. Bioelectron.*, 1992, **7**, 165-185.
193. X. Pang, D. He, S. Luo and Q. Cai, *Sens. Actuators, B*, 2009, **137**, 134-138.
194. Y.-Y. Song, Z. Gao, K. Lee and P. Schmuki, *Electrochem. Commun.*, 2011, **13**, 1217-1220.
195. K.-S. Mun, S. D. Alvarez, W.-Y. Choi and M. J. Sailor, *ACS Nano*, 2010, **4**, 2070-2076.
196. P. R. Solanki, S. Srivastava, M. A. Ali, R. K. Srivastava, A. Srivastava and B. D. Malhotra, *RSC Adv.*, 2014, **4**, 60386-60396.
197. S. S. Mandal, V. Navratna, P. Sharma, B. Gopal and A. J. Bhattacharyya, *Bioelectrochemistry*, 2014, **98**, 46-52.
198. P. Kar, A. Pandey, J. J. Greer and K. Shankar, *Lab on a Chip*, 2012, **12**, 821-828.
199. Y. An, L. Tang, X. Jiang, H. Chen, M. Yang, L. Jin, S. Zhang, C. Wang and W. Zhang, *Chemistry – A European Journal*, 2010, **16**, 14439-14446.
200. R. Wang, C. Ruan, D. Kanayeva, K. Lassiter and Y. Li, *Nano Letters*, 2008, **8**, 2625-2631.
201. Q. Shen, S.-K. You, S.-G. Park, H. Jiang, D. Guo, B. Chen and X. Wang, *Electroanalysis*, 2008, **20**, 2526-2530.
202. L. Tan, Y. Chen, H. Yang, Y. Shi, J. Si, G. Yang, Z. Wu, P. Wang, X. Lu, H. Bai and Y. Yang, *Sens. Actuators, B*, 2009, **142**, 316-320.
203. W.-W. Zhao, Z. Liu, S. Shan, W.-W. Zhang, J. Wang, Z.-Y. Ma, J.-J. Xu and H.-Y. Chen, *Scientific Reports*, 2014, **4**.
204. J. Cui, Y. Ge, S. Chen, H. Zhao, H. Liu, Z. Huang, H. Jiang and J. Chen, *J. Mater. Chem. B*, 2013, **1**, 2072-2077.
205. K. Sunada, T. Watanabe and K. Hashimoto, *J. Photochem. Photobiol., A*, 2003, **156**, 227-233.
206. J. Li, H. Zhou, S. Qian, Z. Liu, J. Feng, P. Jin and X. Liu, *Appl. Phys. Lett.*, 2014, **104**, -.
207. X. Chen, K. Cai, J. Fang, M. Lai, J. Li, Y. Hou, Z. Luo, Y. Hu and L. Tang, *Surf. Coat. Technol.*, 2013, **216**, 158-165.

208. L. Zhao, H. Wang, K. Huo, L. Cui, W. Zhang, H. Ni, Y. Zhang, Z. Wu and P. K. Chu, *Biomaterials*, 2011, **32**, 5706-5716.
209. A. Roguska, A. Belcarz, T. Piersiak, M. Pisarek, G. Ginalska and M. Lewandowska, *Eur. J. Inorg. Chem*., 2012, **2012**, 5199-5206.
210. X. Chen, K. Cai, J. Fang, M. Lai, Y. Hou, J. Li, Z. Luo, Y. Hu and L. Tang, *Colloids Surf., B*, 2013, **103**, 149-157.
211. S.-H. Uhm, D.-H. Song, J.-S. Kwon, S.-B. Lee, J.-G. Han, K.-M. Kim and K.-N. Kim, *Surf. Coat. Technol*., 2013, **228, Supplement 1**, S360-S366.
212. Y. Lai, L. Lin, F. Pan, J. Huang, R. Song, Y. Huang, C. Lin, H. Fuchs and L. Chi, *Small*, 2013, **9**, 2945-2953.
213. H. Li, Q. Cui, B. Feng, J. Wang, X. Lu and J. Weng, *Appl. Surf. Sci*., 2013, **284**, 179-183.